2017

Relative functional and optical absorption cross-sections of PSII and other photosynthetic parameters monitored in situ, at a distance with a time resolution of a few seconds, using a prototype light induced fluorescence transient (LIFT) device

Barry Osmond
University of Wollongong, cosmond@uow.edu.au

Wah Soon Chow
Australian National University (ANU)

Rhys Wyber
University of Wollongong, rwyber@uow.edu.au

Alonso Zavafer
Australian National University

Beat Keller
Forschungszentrum Julich, Gemany

Publication Details

Osmond, B., Chow, W. Soon., Wyber, R., Zavafer, A., Keller, B., Pogson, B. J. & Robinson, S. A. (2017). Relative functional and optical absorption cross-sections of PSII and other photosynthetic parameters monitored in situ, at a distance with a time resolution of a few seconds, using a prototype light induced fluorescence transient (LIFT) device. Functional Plant Biology: an international journal of plant function, 44 (10), 985-1006

See next page for additional authors

Relative functional and optical absorption cross-sections of PSII and other photosynthetic parameters monitored in situ, at a distance with a time resolution of a few seconds, using a prototype light induced fluorescence transient (LIFT) device

Abstract

The prototype light-induced fluorescence transient (LIFT) instrument provides continuous, minimally intrusive, high time resolution (~2 s) assessment of photosynthetic performance in terrestrial plants from up to 2 m. It induces a chlorophyll fluorescence transient by a series of short flashes in a saturation sequence (180 ~1μs flashlets inμs) to achieve near-full reduction of the primary acceptor QA, followed by a relaxation sequence (RQA; 90 flashlets at exponentially increasing intervals over ~30 ms) to observe kinetics of QA re-oxidation. When fitted by the fast repetition rate (FRR) model (Kolber et al. 1998) the QA flash of LIFT/FRR gives smaller values for FmQA from dark adapted leaves than FmPAM from pulse amplitude modulated (PAM) assays. The ratio FmQA/FmPAM resembles the ratio of fluorescence yield at the J/P phases of the classical O-J-I-P transient and we conclude that the difference simply is due to the levels of PQ pool reduction induced by the two techniques. In a strong PAM-analogous WL pulse in the dark monitored by the QA flash of LIFT/FRR φPSIIWL ≈ φPSIIPAM. The QA flash also tracks PQ pool reduction as well as the associated responses of ETR QA → PQ and PQ → PSI, the relative functional (σPSII) and optical absorption (aPSII) cross-sections of PSII in situ with a time resolution of ~2 s as they relax after the pulse. It is impractical to deliver strong WL pulses at a distance in the field but a longer PQ flash from LIFT/FRR also achieves full reduction of PQ pool and delivers φPSIIPQ ≈ φPSIIPAM to obtain PAM-equivalent estimates of ETR and NPQ at a distance. In situ values of σPSII and aPSII from the QA flash with smaller antenna barley (chlorina-f2) and Arabidopsis mutants (asLhcb2-12, ch1-3 Lhcb5) are proportionally similar to those previously reported from in vitro assays. These direct measurements are further validated by changes in antenna size in response to growth irradiance. We illustrate how the QA flash facilitates our understanding of photosynthetic regulation during sun flecks in natural environments at a distance, with a time resolution of a few seconds.

Disciplines

Medicine and Health Sciences | Social and Behavioral Sciences

Publication Details

Osmond, B., Chow, W. Soon., Wyber, R., Zavafer, A., Keller, B., Pogson, B. J. & Robinson, S. A. (2017). Relative functional and optical absorption cross-sections of PSII and other photosynthetic parameters monitored in situ, at a distance with a time resolution of a few seconds, using a prototype light induced fluorescence transient (LIFT) device. Functional Plant Biology: an international journal of plant function, 44 (10), 985-1006

Authors

Barry Osmond, Wah Soon Chow, Rhys Wyber, Alonso Zavafer, Beat Keller, Barry Pogson, and Sharon A. Robinson

Publisher: CSIRO; Journal: FP:Functional Plant Biology
Article Type: research-article; Volume: ; Issue: ; Article ID: FP17024
DOI: 10.1071/FP17024; TOC Head:

Relative functional and optical absorption cross-sections of PSII and other photosynthetic parameters monitored *in situ*, at a distance with a time resolution of a few seconds, using a prototype light induced fluorescence transient (LIFT) device

Barry Osmond[A,B,D], *Wah Soon Chow*[B], *Rhys Wyber*[A], *Alonso Zavafer*[B], *Beat Keller*[C], *Barry J. Pogson*[B] *and Sharon A. Robinson*[A]

[A]Centre for Sustainable Ecosystem Solutions, School of Biological Sciences, University of Wollongong, Northfields Avenue, Wollongong, NSW 2522, Australia.

[B]Division of Plant Sciences, Research School of Biology, Australian National University, Acton, ACT 2601, Australia.

[C]Institute of Bio- and Geosciences, IBG-2: Plant Sciences, Forschungszentrum Jülich GmbH, 52425 Jülich, Germany.

[D]Corresponding author. Email: osmond.barry@gmail.com

The prototype light-induced fluorescence transient (LIFT) instrument provides continuous, minimally intrusive, high time resolution (~2 s) assessment of photosynthetic performance in terrestrial plants from up to 2 m. It induces a chlorophyll fluorescence transient by a series of short flashes in a saturation sequence (180 ~1μs flashlets in <500 μs) to achieve near-full reduction of the primary acceptor Q_A, followed by a relaxation sequence (RQ_A; 90 flashlets at exponentially increasing intervals over ~30 ms) to observe kinetics of Q_A re-oxidation. When fitted by the fast repetition rate (FRR) model (Kolber *et al*. 1998) the Q_A flash of LIFT/FRR gives smaller values for F_mQ_A from dark adapted leaves than F_mPAM from pulse amplitude modulated (PAM). The ratio F_mQ_A/F_mPAM resembles the ratio of fluorescence yield at the J/P phases of the classical O-J-I-P transient and we conclude that the difference simply is due to the levels of PQ pool reduction induced by the two techniques. In a strong PAM-analogous WL pulse in the dark monitored by the Q_A flash of LIFT/FRR $\phi_{PSII}WL \approx \phi_{PSII}PAM$. The Q_A flash also tracks PQ pool reduction as well as the associated responses of ETR $Q_A \rightarrow$ PQ and PQ $\rightarrow$ PSI, the relative functional (σ_{PSII}) and optical absorption (a_{PSII}) cross-sections of PSII *in situ* with a time resolution of ~2 s as they relax after the pulse. It is impractical to deliver strong WL pulses at a distance in the field but a longer PQ flash from LIFT/FRR also achieves full reduction of PQ pool and delivers $\phi_{PSII}PQ \approx \phi_{PSII}PAM$ to obtain PAM-equivalent estimates of ETR and NPQ at a distance. *In situ* values of σ_{PSII} and a_{PSII} from the Q_A flash with smaller antenna barley (*chlorina-f2*) and *Arabidopsis* (*asLhcb2–12*, *ch1–3 Lhcb5*) mutants are proportionally similar to those previously reported from *in vitro* assays. These direct measurements are further validated by changes in antenna size in response to growth irradiance. We illustrate how the Q_A flash facilitates our understanding of photosynthetic regulation during sun flecks in natural environments at a distance, with a time resolution of a few seconds.

Additional keywords: *Arabidopsis* mutants, avocado, barley mutants, electron transfer rates, NPQ, O-J-I-P transient.

Publisher: CSIRO; Journal: FP:Functional Plant Biology
Article Type: research-article; Volume: ; Issue: ; Article ID: FP17024
DOI: 10.1071/FP17024; TOC Head:

A new approach to monitoring leaf photosynthesis in situ using 30 ms chlorophyll fluorescence transients at ~ 2 s intervals at distances up to 2 m is described. By monitoring fluorescence with near full reduction of Q_A (the primary quinone acceptor of PSII) these transients deliver parameters not directly available from other methods (relative functional absorption cross section of photosystem II, rates of intersystem electron transport and relative oxidation state the plastoquinone (PQ) pool). These permit non-intrusive evaluation of brief sun flecks in shade canopies whereas calibration against traditional PAM methods is obtained in longer protocols achieving full reduction of PQ.

Introduction

Observations of chlorophyll fluorescence transients in plants by Kautsky and Hirsch (1931) and MacAlister and Myers (1940) continue to inspire development of optical approaches to measuring photosynthetic processes (Briantais *et al*. 1979; Bradbury and Baker 1981; Schreiber *et al*. 1986; Krause and Weis 1991; Govindjee 1995; Maxwell and Johnson 2000; Baker 2008). The perceptive assessment of Lavorel and Etienne (1977) that chlorophyll fluorescence *in situ* is 'both a rich and ambiguous signal' that is 'no longer a subject for specialists alone' marks a turning point in the adoption of this approach for the integration of light and dark reactions of photosynthesis. For example, Walker (1981) associated of the secondary S-M-T transients of chlorophyll fluorescence emission (Papageorgiou and Govindjee 1968) with his studies of oscillatory features of photosynthetic oxygen evolution and carbon metabolism during induction. Walker *et al*. (1984) suggested that 'we can even stride, without lingering more than a few milliseconds, through the photochemical era into the patterns of successive waves of fluorescence which constitute the Kautsky effect'.

The introduction of pulse amplitude modulated (PAM) measurements of chlorophyll fluorescence (Schreiber *et al*. 1986) transformed our understanding of transient photosynthetic processes *in situ* and facilitated its applications to plant ecophysiology. A further two decades later, this transformation was acknowledged when Uli Schreiber was awarded the inaugural Innovation Prize from the International Society for Photosynthesis Research at its 14th International Congress in Glasgow in 2007. By that time, spot measurements with hand-held, on-the-leaf PAM measurement systems had been used to elucidate photosynthetic responses to drought in canopy dominants (Rascher *et al*. 2004) by rope climbers suspended throughout the ~15 m deep 1900 m^2 lowland tropical rainforest biome in an enclosed 35000 m^3 controlled environment at the Biosphere 2 Laboratory (B2 L) in Oracle AZ, USA (Leigh *et al*. 1999). Monitoring-PAM (Porcar Castell *et al*. 2008) and similar devices notwithstanding, it is impractical to apply PAM-like saturating pulses at a distance. The requirement to perform PAM measurements near the leaf surface limits the application of this method in less accessible locations typical of natural terrestrial environments. Although initial steps to integrate PAM with LIDAR and telescopic capture of chlorophyll fluorescence (Chappelle *et al*. 1984) for close range (<2 m) monitoring of leaf water stress (Cerovic *et al*. 1996; Flexas *et al*. 2000; Ounis *et*

Publisher: CSIRO; Journal: FP:Functional Plant Biology
Article Type: research-article; Volume: ; Issue: ; Article ID: FP17024
DOI: 10.1071/FP17024; TOC Head:

al. 2001) seem promising, the intrusive nature of the saturating pulse limits the frequency of data acquisition to ~30–60 s.

Since Kolber and Falkowski (1993), fast repetition rate (FRR) fluorometers have been widely used to assess photosynthetic performance of phytoplankton *in situ* and extensively calibrated against gas exchange and PAM methods (Melrose *et al*. 2006; Suggett *et al*. 2009). The first two versions of terrestrial LIFT/FRR instruments that employed eye-safe red laser diodes as excitation sources, with a working range of 10–40 m also were empirically calibrated against gas exchange and PAM (Ananyev *et al*. 2005; Kolber *et al*. 2005; Pieruschka *et al*. 2010, 2014; Nichol *et al*. 2012). Advances in oceanographic applications (Oxborough *et al*. 2012) remain closely relevant to terrestrial studies but, in general, *in situ* measurements of functional and optical absorption cross-sections of PSII and other parameters using FRR are rarely mentioned in overviews of chlorophyll fluorescence (e.g. Kalaji *et al*. 2017).

Although similar in terms of the PSII phenomena detected, the PAM and LIFT/FRR assays differ in their measurement and monitoring approaches to assessment of chlorophyll fluorescence. In general terms, on-the-leaf PAM systems use a modulated weak measuring beam to establish the minimum level of chlorophyll fluorescence before applying a brief (e.g. 0.8 s) saturating pulse of white light (WL) in the dark to fully reduce the PQ pool, close all PSII centres and achieve maximum fluorescence yield. The maximum photochemical efficiency of PSII is then calculated from the ratio of variable fluorescence to maximum fluorescence. In actinic light, subsequent saturating pulses are used to estimate overall linear ETR (Genty *et al*. 1989) and NPQ (Bilger and Björkman 1990), with a time resolution of ~30 s.

In contrast, LIFT/FRR uses the excitation and data fitting protocols previously developed for oceanographic research (Kolber *et al*. 1998; Gorbunov *et al*. 2000). These employ a sequence of short (1 μs), high frequency subsaturating flashlets to induce a fluorescence transient in <1 ms that is specifically designed to progressively reduce Q_A before electron transfer to the PQ pool (the SQ_A phase of the Q_A flash). This is followed by a 30 ms relaxation sequence with weaker flashlets applied at exponentially increasing intervals to monitor the kinetics of Q_A reoxidation during electron transfer to PSI (the RQ_A phase of the Q_A flash). The raw fluorescence transient data are fitted by the FRR model to estimate initial F_oQ_A and F_mQ_A, and to calculate the variable component of fluorescence F_vQ_A (Table 1). In addition, this model gives access to a range of fundamental PSII properties and ETR parameters, such as functional and optical absorption cross-section of PSII, the kinetics of photosynthetic electron transport between PSII and PSI, and the relative oxidation state of the PQ that until recently, were not directly available from other methods.

Here we emphasise that the Q_A flash protocol of LIFT/FRR is a minimally intrusive method for monitoring photosynthetic performance of terrestrial plants. At the outset we seek to remove, as far as possible, the ambiguity associated with the abbreviations used to report chlorophyll fluorescence data

Publisher: CSIRO; Journal: FP:Functional Plant Biology
Article Type: research-article; Volume: ; Issue: ; Article ID: FP17024
DOI: 10.1071/FP17024; TOC Head:

from LIFT/FRR and PAM (Table 1) and then explore six distinctive attributes of LIFT/FRR. First, as generally observed in comparisons of the two methods with leaves (Ananyev *et al*. 2005) and in marine systems (Suggett *et al*. 2003, 2009), values of F_mQ_A are lower than those of F_mPAM, which, if not calibrated and corrected, generate lower values of ETR and higher values of NPQ than PAM. In seeking a better understanding of this difference we note the comment by Falkowski and Kolber (1995) that 'the FRR method is, in effect, a fluorescence induction curve within ~150 μs' and so compare the fluorescence yields of LIFT/FRR with those at different steps in the traditional O-J-I-P induction curve. Without wishing to engage deeply with the longstanding and detailed dissection of chlorophyll fluorescence induction *in situ* (Duysens and Sweers 1963; Strasser *et al*. 1995; Stirbet and Govindjee 2012; Schansker *et al*. 2014; Vredenberg 2015; Kalaji *et al*. 2017), we hypothesise that the difference in fluorescence yield and variable fluorescence from the Q_A flash of LIFT/FRR and PAM simply is due to the levels of PQ pool reduction induced by the two techniques.

Second, because it is impracticable to deliver strong WL pulses at a distance, we follow Kolber *et al*. (1998) and adopt a longer PQ flash from LIFT/FRR that achieves full reduction of the PQ pool and yields values of $\phi_{PSII}PQ \approx \phi_{PSII}PAM$. When deployed after a Q_A flash as a 'double flash', or at intervals in a Q_A flash train, the PQ flash serves as a reference for PAM-equivalent estimates of ETR and NPQ. Third, we show that the Q_A flash gives PAM-equivalent estimates of ϕ_{PSII} during a PAM-analogous strong WL pulse in the dark but in addition, monitors relaxation of the pulse-induced over reduction of the PQ pool, perturbations of ETR parameters and functional (σ_{PSII}) and optical (a_{PSII}) cross-sections of PSII. Fourth, we show that continuous monitoring of photosynthetic parameters by LIFT/FRR with a time resolution of a few seconds is much less intrusive than PAM. Fifth, we validate the LIFT/FRR estimates of the relative sizes of σ_{PSII} and a_{PSII} against well established *in vitro* estimates of antenna size between wild types and mutants of barley and *Arabidopsis*. Sixth and finally, we illustrate the potential of these minimally intrusive LIFT/FRR capabilities to advance our understanding mechanisms of photosynthetic regulation in highly variable irradiance (sun fleck) regimes in the field, with a time resolution of a few seconds.

Our emphasis on the *in situ* measurement of functional and optical absorption cross-sections of PSII with the Q_A flash as an integrative approach to fundamental relationships between energy conversion and light harvesting phenomena is timely. Clearly, PAM techniques are also evolving towards measurements of these parameters, albeit based on different assumptions and methodology (Klughammer and Schreiber 2015). As noted previously, the LIFT and PAM approaches seem to be 'converging to provide an increasingly consistent picture of photosynthesis fluorescence relationships' (Schreiber *et al*. 2012). To this end, we present chlorophyll fluorescence data acquired with the prototype blue LED LIFT, augmented by insights from traditional on the leaf O-J-I-P induction curves and comparative PAM measurements. Our overall goal is to demonstrate the feasibility of continuous, minimally intrusive monitoring of novel photosynthetic parameters in

Publisher: CSIRO; Journal: FP:Functional Plant Biology
Article Type: research-article; Volume: ; Issue: ; Article ID: FP17024
DOI: 10.1071/FP17024; TOC Head:

leaves at a distance, with high time resolution, potentially guiding future applications of LIFT/FRR to advance our understanding of plant responses to stochastic elements of the natural light environment.

Materials and methods

Plant material

A variety of plant material has been examined using the prototype LIFT/FRR system. Initially, plants with large, planar leaves were selected for adjacent comparison of LIFT and PAM assays under the same incident actinic light treatments. Spinach (*Spinacea oleracea* L.) was grown under shade cloth (15% outdoor PFD; peak ~300 µmol photons m^{-2} s^{-1}) and in full sunlight (65% outdoor PFD; peak ~1300 µmol photons m^{-2} s^{-1}) in a south facing temperature controlled greenhouse (25°C day/15°C night) at the Research School of Biology, Australian National University (RSB, ANU). Cotton (*Gossypium hirsutum* L.) was grown in sunlight in the same greenhouse. Avocado (*Persea americana* Mill.) was grown from seed in this greenhouse and transferred to the shaded area for at least 6 months before use. Other avocado plants were grown indoors in a stairwell atrium in the Research School of Chemistry, ANU. The rubber plant (*Ficus elastica* Roxb. ex Hornem.), was grown in a high humidity and heavily shaded tropical greenhouse (peak ~80 µmol photons m^{-2} s^{-1}). Barley (*Hordeum vulgare* L.) and its chlorophyll (Chl) *b*-less mutant (*chlorina-f2*, Highkin 1950; deficient in several LHCIIs, Bossmann *et al*. 1997) were grown in full greenhouse sunlight in Canberra, and the same seed batches were batches grown in a greenhouse with supplementary lighting (80–400 µmol photons m^{-2} s^{-1}, average ~100 µmol photons m^{-2} s^{-1} with 16 h day/8h night) at Forschungszentrum Jülich, Germany (FzJ).

Arabidopsis thaliana (L.) Heynh. genotypes were cultivated in controlled environment growth chambers (20°C at ~80 and ~120 µmol photons m^{-2} s^{-1}) at RSB, ANU. Wild-type *Col*, as well as NPQ mutants *npq-1* (violaxanthin de-epoxidase deficient; Niyogi *et al*. 1998), *npq*-4 (ΔpH sensing PsbS protein deficient; Li *et al*. 2002) were grown. Two classes of state transition mutants were examined: *asLhcb2–12* (almost completely devoid of Lhcb1 and Lhcb2; Andersson *et al*. 2003) and Chl *b*-depleted *chl-3 Lhcb5* (Kim *et al*. 2009), as well as the *STN7* and *STN 7/8* kinase mutants *stn7* (Tikkanen *et al*. 2006) and *stn7/8* (Bonardi *et al*. 2005).

The prototype LIFT apparatus

The first two versions of terrestrial LIFT/FRR instruments employed red laser diodes as excitation sources, with a working range of 10–40 m (Ananyev *et al*. 2005; Kolber *et al*. 2005; Pieruschka *et al*. 2010, 2014). Unfortunately, use of lasers in terrestrial environments faces progressively restrictive regulations due to legitimate eye safety concerns. Emergence of increasingly powerful light emitting diodes (LEDs) allowed application of non-coherent (thus much safer) light sources with LIFT instrumentation, but at a cost of substantially lower operating range. Nevertheless, the advantages of continuous, remote measurements of a range of photosynthetic characteristics far outweigh this

Publisher: CSIRO; Journal: FP:Functional Plant Biology
Article Type: research-article; Volume: ; Issue: ; Article ID: FP17024
DOI: 10.1071/FP17024; TOC Head:

limitation and commercial versions of the device used here are now available (http://www.soliense.com/LIFT_Terrestrial.php, accessed 10 May 2017).

The prototype limited-range LIFT/FRR instrument used here comprises a custom-built excitation unit with a fibre-optic emission collector at the focal point of a 120 mm aperture, 130 mm focal length custom-built telescope. The telescope projects blue light (BL; 470 nm) from a LED (Luxeon LXML-PB02–0070) onto the target leaf providing both the fast repetition rate (FRR) excitation pulses (Kolber *et al*. 1998) as well as DC actinic illumination when required. The excitation light is focused on a 3 × 4 cm target at 60–120 cm distance using manual adjustment of the focal point to constrain changes in the excitation power at varying distance. Due to the low aperture/focal length ratio, the excitation power remains relatively stable within ±10 cm range (the commercial LIFT instrument is equipped with a motorised, software-controlled adjustment of the focal point, and operates with a pre-calibrated table of the excitation power within the instrument operating range). The same telescope collects the red chlorophyll fluorescence signal, separated from the BL with a 45-degree red-reflecting dichroic mirror (Edmund Optics NT47–948) and conveyed by a 12.5 mm diameter flexible, 1 m long optical fibre to the detector unit of a conventional bench-top FRRF system used in marine applications (http://www.soliense.com/LIFT_Marine.php, accessed 10 May 2017). A 685 nm interference filter (25 nm bandwidth, 75% transmission; custom-made by Intor Inc.) separates the red chlorophyll fluorescence emission from the blue reflected excitation light.

The system is operated with a modified version of the FRR fluorescence saturation/relaxation protocol (Kolber *et al*. 1998; Kolber *et al*. 2005). The number of flashlets, their energy and frequency are controlled by the LIFT software, with FRR analysis of the fluorescence transients adjusted to optimise observations of plants under investigation. In the experiments reported here the excitation light source delivers short pulses (flashlets) of 470 nm light (peak excitation power of 12 600 μmol photons m^{-2} s^{-1}), each activating ~2–4% of PSII reaction centres while exciting a chlorophyll fluorescence signal (i.e. simultaneously performing both actinic and monitoring functions). Two excitation protocols are used, both of which comprised saturation and relaxation phases. The first one, the Q_A flash, continuously monitors maximum chlorophyll fluorescence emission with ~90% reduction of Q_A and <10% reduction of the PQ pool (http://www.soliense.com/LIFT_Method.php). The second, the PQ flash is applied for spot measurements to determine maximum fluorescence yield under conditions of fully reduced Q_A and PQ pool.

Notation for LIFT/FRR chlorophyll fluorescence parameters

Table 1 summarises the notation used for data collected and processed by the LIFT/FRR technique. This notation is needed to clarify differences between specific LIFT/FRR fluorescence parameters and to remove potential ambiguity in currently accepted nomenclature when comparing these data with those acquired from the saturating pulse of PAM systems. The Q_A postfix in LIFT/FRR parameters indicates that they were obtained by processing Q_A flash transients,

Publisher: CSIRO; Journal: FP:Functional Plant Biology
Article Type: research-article; Volume: ; Issue: ; Article ID: FP17024
DOI: 10.1071/FP17024; TOC Head:

numerically extrapolated to conditions of nearly full reduction of Q_A. Data from three other assays that provide estimates of fluorescence yield under conditions of full reduction of both Q_A and the PQ pools are distinguished. The postfix *WL* identifies fluorescence signals from the Q_A flash obtained during an externally applied, PAM-analogous ~1 s pulse of strong WL. Another longer LIFT/FRR protocol, also designed to achieve full reduction of Q_A and the PQ pool is identified by the postfix *PQ*. Signals obtained on the leaf with PAM systems are differentiated by the postfix *PAM*. This specific, complex nomenclature is also adopted to distinguish LIFT/FRR protocols from the ST (single turnover) and MT (multiple turnovers) designations of micro algal FRR protocols (Kolber *et al*. 1998; Oxborough *et al*. 2012), and to avoid confusion when monitoring state transitions (abbreviated to ST) with LIFT/FRR as reported in subsequent publications.

The Q_A flash protocol

The Q_A flash is designed to reduce Q_A irrespective of the state of reduction (or oxidation) of the PQ pool, thus allowing measurement of intrinsic PSII and electron transport parameters which are otherwise susceptible to modification by the redox state of the PQ pool. In the prototype used here the Q_A flash comprises a saturation sequence (SQ_A; Fig. 1*a*) of 180 flashlets at 50% duty cycle (average excitation power of ~6300 µmol photons m^{-2} s^{-1}: 1 µs pulses of light applied at 2.0 µs intervals, corresponding to phase I of the ST1 flash; Kolber *et al*. 1998). As the rate of excitation delivery to PSII reaction centres during the SQ_A phase far exceeds the rates of Q_A re-oxidation, the level of Q_A reduction progressively increases from flashlet-to-flashlet, reaching ~90% within ~360 µs. The fluorescence signal increases proportionally in response to the level of Q_A reduction (Fig. 1*a*), with a slope defined by the excitation power, the efficiency of photosynthetic light utilisation by PSII, and by concurrent rates of photosynthetic electron transport (ETR). The acquired fluorescence transients are iteratively fitted to the FRR model to obtain parameter values listed in Table 1, as described below.

The Q_A re-oxidation kinetic is then followed over the next ~30 ms using 90 flashlets (Fig. 1*a*, *b*) applied at exponentially increasing time intervals (RQ_A; corresponding to phase II of the ST1 flash; Kolber *et al*. 1998). The decrease in excitation power shifts the equilibrium between rates of excitation delivery and the rates of electron transport towards the latter. As a result, the observed fluorescence yield decreases with kinetics initially defined by the rates of electron transport from Q_A to the PQ pool, and subsequently by electron transport from the PQ pool to PSI. The decline in fluorescence yield during RQ_A is fitted by two exponentials (τ_1 and τ_2) corresponding to the half times for electron transfer from Q_A to the PQ pool, and from the PQ pool to PSI respectively.

The PQ flash and 'double flash' protocols

The PQ flash is designed as a prolonged saturation sequence (SPQ, up to 6000 flashlets at 5% duty cycle; ~630 µmol photons m^{-2} s^{-1} over ~120 ms) to achieve full reduction of the PQ pool (Fig. 2*a*; corresponding to MT, phase III; Kolber *et al*. 1998), thereby facilitating comparisons with PAM data.

Publisher: CSIRO; Journal: FP:Functional Plant Biology
Article Type: research-article; Volume: ; Issue: ; Article ID: FP17024
DOI: 10.1071/FP17024; TOC Head:

The lower excitation power and longer duration of the PQ flash causes gradual reduction of the PQ pool, resulting in progressively slower rates of Q_A^- re-oxidation. With fully reduced PQ pool these rates slow ~5–10 times and become limited by the rates of electron transport from the PQ pool to PSI that can be tracked during a second relaxation phase (RPQ) of 90 flashlets (Fig. 2*b*; corresponding to the MT flash phase IV; Kolber *et al*. 1998).

The change in the equilibrium between rates of excitation delivery and electron transport dramatically changes the character of fluorescence saturation during the PQ flash, with the initial phase representing partial Q_A reduction in the presence of fast electron transport from Q_A to the PQ pool, and the second phase resulting in full Q_A reduction under conditions of decelerated $Q_A \rightarrow$ PQ electron transport due to progressive PQ pool reduction. Effectively, the PQ flash achieves full reduction of the PQ pool, i.e. $F_oPQ \approx F_mPQ$. Although the numerical values of F_mPQ and F_mPAM differ depending on instrument settings, F_vPQ/F_mPQ and F_vPAM/F_mPAM yield comparable estimates of the maximum attainable photochemical efficiency of PSII. It is convenient to represent these parameters as $\phi_{PSII}PQ$ and $\phi_{PSII}PAM$ with corresponding values obtained in the light as $\phi'_{PSII}PQ$ and $\phi'_{PSII}PAM$ (Table 1).

The Q_A and PQ flashes can be applied in quick succession in a protocol termed a ‘double flash’ (Fig. 2*a, b*) allowing immediate measurement of the fluorescence yield (and photochemical efficiencies of PSII) associated with selective reduction of the Q_A and PQ pools. This protocol provides a convenient internal calibration of F_mQ_A against F_mPQ in the same target tissue with the same optical path, thus allowing direct comparison between $\phi_{PSII}Q_A$ and $\phi_{PSII}PQ$ and facilitating calibration of $\phi_{PSII}Q_A$ against $\phi_{PSII}PAM$. In addition, the PQ flash is readily programmed to fire at predetermined intervals (e.g. every 60 s) giving reference estimates of $\phi'_{PSII}PQ$ while continuously monitoring $\phi'_{PSII}Q_A$ in the course of actinic induction or light response curves. In general, the remotely delivered PQ flash provides an important reference for high time resolution estimates of PAM equivalent overall ETR and NPQ in the field.

In the laboratory it is convenient to continuously monitor F_mQ_A at 2 s intervals before, during and after a PAM-analogous strong pulse of WL (~1 s, ~2000 μmol photons m^{-2} s^{-1}) from an external quartz-iodide lamp to calibrate lower values of F_mQ_A with larger values of F_mWL and F_mPAM. The strong WL pulse achieves full reduction of the PQ pool (as indicated by elimination of F_vQ_A; $\phi'_{PSII}Q_A \approx 0$ during the pulse). This provides a PAM-equivalent reference ($F_mWL \approx F_mPAM$) for assays of ETR and NPQ responses before actinic treatments. As with PAM, it is impractical to deliver such strong WL pulses in the field where the PQ flash and ‘double flash’ serve the same purpose.

Publisher: CSIRO; Journal: FP:Functional Plant Biology
Article Type: research-article; Volume: ; Issue: ; Article ID: FP17024
DOI: 10.1071/FP17024; TOC Head:

Data processing and estimates of functional (σ_{PSII}) and optical (a_{PSII}) absorption cross-section, and simulation of E_k (half saturation PFD for ETR)

The fluorescence transients produced by the Q_A flash are numerically fitted to the FRR model with a custom-designed application software package that describes the relationship between the excitation power, fluorescence yield, and PSII photosynthetic properties (Kolber *et al*. 1998; http://soliense.com//LIFT_Method.php, accessed 10 May 2017). The FRR fitting procedure allows calculation of F_oQ_A or $F'Q_A$ (initial fluorescence yield before Q_A flash) and F_mQ_A or F'_mQ_A (the fluorescence yield corresponding to fully-reduced Q_A). The difference between F_mQ_A and F_o is used to calculate $\phi_{PSII}Q_A = (F_mQ_A - F_o)/F_mQ_A$, the estimate of maximum photochemical efficiency of PSII in the dark. The difference between F'_mQ_A and F' measured in the light is used to calculate $\phi'_{PSII}Q_A = (F'_mQ_A - F')/F'_mQ_A)$, the estimate of photochemical efficiency of PSII at the prevailing level of ambient illumination. Parameters $\phi_{PSII}Q_A$ and $\phi'_{PSII}Q_A$ from the Q_A flash differ from those assessed from the saturating pulse of PAM or from the LIFT/FRR PQ flash by a factor determined by the level of PQ pool reduction before application of the Q_A flash. As shown later, F_mQ_A values assessed under conditions of oxidised PQ pool are 30–40% lower than the LIFT F_mPQ and PAM F_m values, resulting in 10–15% lower values $\phi_{PSII}Q_A$ derived from the Q_A flash.

The FRR fitting procedure also extracts the time constants for electron transport $Q_A \rightarrow$ PQ pool (τ_1) and PQ pool $\rightarrow$ PSI (τ_2) from the RQ_A phase of the Q_A flash (Fig. 1*b*) and computes the relative oxidation status of the PQ pool, all of which are based on fitting the entire LIFT fluorescence transient with the FRR model. Likewise, the model also computes σ_{PSII} (the functional absorption cross-section of PSII) that is to a first degree, given by the initial slope of the Q_A flash transient (Fig. 1*a*). With the prototype LIFT/FRR system described here, the Q_A flash applied at rates of up to one flash every 2–3 s allows continuous monitoring of σ_{PSII} and σ'_{PSII} (functional absorption cross-sections of PSII in the dark and in the light respectively). This parameter defines efficiency of photosynthetic light utilisation, a composite measure of light absorption, excitation transfer, and photosynthetic charge separation. Aside from its intrinsic value, this direct, *in situ* estimate of σ_{PSII} is central to FRR-based estimates of two other parameters.

First, measurements of σ_{PSII} are used to estimate optical absorption cross-section (a_{PSII}, in units of $Å^2$/PSII centre) that quantifies the PSII-specific rates of light absorption and provides an 'apparent' measure of PSII antenna size *in situ*. As shown previously $a_{PSII} = \sigma_{PSII}/\phi_{PSII}$ (Kolber *et al*. 1998 refer to equation 12, derived from equations 7–9). We assume that ϕ_{PSII} remains constant under actinic light and calculate as $a'_{PSII} = \sigma'_{PSII}/\phi_{PSII}$, using ϕ_{PSII} measured during dark periods. Although this assumption is generally valid under subsaturating irradiances, it doesn't hold under high light conditions, where closed PSII traps decrease the overall ϕ_{PSII} averaged over open and closed PSII traps.

Publisher: CSIRO; Journal: FP:Functional Plant Biology
Article Type: research-article; Volume: ; Issue: ; Article ID: FP17024
DOI: 10.1071/FP17024; TOC Head:

Second, together with simultaneously-assessed kinetics of electron transport, σ_{PSII} is used to estimate the initial slope of electron transport rates as a function of irradiance (α_o) and the saturated rate of overall electron transport between PSII and PSI (ETR_{max}). The estimated α_o is wavelength-dependent, and in our case, it reflects the initial slope of ETR at 470 nm. Nevertheless, it can be used to infer relative changes in this parameter under ambient irradiance. The half-saturation irradiance of photosynthetic electron transport (E_k) is then estimated as $E_k = ETR_{max}/\alpha_o$. This parameter is of interest when investigating transient photosynthetic responses to fluctuating light and for quantifying changes in light use efficiency associated with thermal dissipation of excitation energy following induction of NPQ *in situ*.

Other measurements

Assuming that the Q_A flash produces nearly-full reduction of Q_A, the ratio of F_mQ_A to F_mPQ should resemble the ratio of fluorescence yield attained at phase J to that of maximum yield attained at P in the course of fast O-J-I-P chlorophyll fluorescence induction transients (Strasser *et al*.1995). To test this assumption, the M-PEA instrument (Hansatech Instruments) was used with 625 nm excitation (6000 μmol photons m^{-2} s^{-1}) to make O-J-I-P measurements on spinach leaves. All the PAM data reported here were obtained with the MINI-PAM system (Heinz Walz GmbH) with settings optimised to obtain comparable fluorescence yields with LIFT/FRR measurements. Light intensity measurements were made with the ULM-500 light meter using calibrated MSQ-B and LS-C PAR sensors from the same supplier. A Skye sensor (SKP 216-ER sensor; 550–750 nm, Skye Instruments) was used to measure 740 nm light. Pigment analyses were done as described previously (Jia *et al*. 2013).

Results

Compared with the large laser-powered LIFT/FRR instruments successfully applied to continuously monitor ETR and NPQ in canopies at a distance in controlled environments and at secure field sites (Ananyev *et al*. 2005; Kolber *et al*. 2005; Pieruschka *et al*. 2010, 2014) the prototype smaller eye-safe instrument described here is suited for photosynthesis research in general, in the laboratory and the in the field, at a distance <2 m. We need to address, however, the fact that values of F_mQ_A and $\phi_{PSII}Q_A$ from the Q_A flash of this and other LIFT/FRR instruments are smaller than those obtained from the saturating pulse of PAM. If not cross calibrated, values of F_mQ_A generate higher estimates of NPQ and $\phi_{PSII}Q_A$ generates lower ETR than PAM.

Presumably this difference in maximum fluorescence yield arises because the brief (~0.5 ms) Q_A flash measures PSII fluorescence with nearly fully reduced Q_A, with little effect on the state of PQ pool reduction, in contrast to the long (0.5–1.0 s) saturating white light pulse of PAM that achieves full reduction of the PQ pool. This difference is readily appreciated by comparisons with fluorescence yields at steps O, J and P in the traditional O-J-I-P chlorophyll *a* fluorescence induction transient (Fig. 3). Although interpretations of many components of the O-J-I-P transient remain complex

Publisher: CSIRO; Journal: FP:Functional Plant Biology
Article Type: research-article; Volume: ; Issue: ; Article ID: FP17024
DOI: 10.1071/FP17024; TOC Head:

(Stirbet and Govindjee 2012; Schansker *et al*. 2014; Vredenberg 2015; Kalaji *et al*. 2017), it is generally agreed that the initial O-J component corresponds to photochemical processes related to reduction of Q_A, the primary electron acceptor of PSII, whereas the J-I-P phase (the so called thermal phase) reflects further increases in the fluorescence signal related to progressive reduction of the PQ pool. Despite the variability in absolute values of fluorescence yield during O-J-I-P (due to variability between leaves and assay parameters), the lower values of F_mQ_A compared with F_mPAM (or F_mPQ, or F_mWL from LIFT) should reflect the ratios of fluorescence yield at J compared with those at P measured with the M-PEA instrument (Fig. 3).

With dark adapted, greenhouse-grown spinach the fluorescence yield at J (at 1.9 ms) is only 55 ± 5% (n = 6) of that at P (at 300 ms). This is similar to ratios of fluorescence yields from the Q_A flash of LIFT/FRR; the yields of F_mQ_A are 63 ± 1% (n = 9) of those from the PQ flash (F_mPQ) in 'double flash' measurements on the same spinach leaves (Fig. 2). Other 'double flash' measurements with shade-grown spinach give values of F_mQ_A that were 56 ± 2% (n = 17) of F_mPQ, and in shade-grown avocado F_mQ_A is 69 ± 1% (n = 18) of F_mPQ. Likewise, in nine *Arabidopsis* genotypes F_mQ_A was 59 ± 1% of F_mWL (n = 41). In general terms, the lower values of F_mQ_A from LIFT/FRR are consistent with accepted interpretations of the O-J phase of the O-J-I-P transient, and measure PSII fluorescence yield with nearly fully reduced Q_A, before substantial electron transfer to PQ. Moreover, the spinach leaves measured in the OJIP assays have $\phi_{PSII}Q_A$ (0.746 ± 0.013; n = 9) that is 89% of $\phi_{PSII}PQ$ (0.839 ± 0.009; n = 9) and in shade leaves of avocado $\phi_{PSII}Q_A$ (0.691 ± 0.003; n = 18) is 87.5% of $\phi_{PSII}PQ$ (0.790 ± 0.003; n = 18). In the nine *Arabidopsis* genotypes $\phi_{PSII}Q_A$ (0.720 ± 0.003; n = 41) is 86.4% of $\phi_{PSII}WL$ (0.833 ± 0.004; n = 41) and 90% of $\phi_{PSII}PAM$ (0.798 ± 0.002; n = 22).

We observe that the increased fluorescence yield monitored by the Q_A flash during a strong WL pulse (below) and measured in the PQ flash of LIFT/FRR (Fig. 2*a, b*) corresponds to the increases measured during the J-I-P phases of the O-J-I-P transient (Fig. 3). We suggest that the principal factor responsible for the difference between the LIFT/FRR Q_A flash based measurements and PAM-based measurements is the level of PQ pool reduction that is attained during the respective assays. This interpretation is implicit in the original description of the FRR technique (Kolber *et al*. 1998) and recognises that 'full reduction of Q_A is a necessary, but not sufficient' (Stirbet and Govindjee 2012) prerequisite for the maximum fluorescence signal. Further speculation as to the multitude of forward and backward photochemical processes that may determine the extent of Q_A reduction achieved during the Q_A flash and sources of the additional fluorescence associated with full reduction of the PQ pool is relegated to the discussion.

Estimating the functional and optical absorptions of PSII, ETR parameters and relative PQ pool oxidation status from the Q_A flash during and after a PAM-equivalent strong WL pulse in the dark

These capabilities are illustrated by Q_A flash analysis of the impact of a strong WL pulse (~1 s) in the dark (Fig. 4) in *Arabidopsis* NPQ mutant; *npq*-4 (NPQ impaired by antisense to the ΔpH sensing

Publisher: CSIRO; Journal: FP:Functional Plant Biology
Article Type: research-article; Volume: ; Issue: ; Article ID: FP17024
DOI: 10.1071/FP17024; TOC Head:

PsbS protein, Li *et al*. 2002). The FRR fitted data from Q_A flashes (Fig. 4*a–e*) and Q_A flash transients at selected colour-coded time points (Fig. 4*a*) before and after the WL pulse (Fig. 4*f–h*), show dramatic effects of the strong WL pulse extending for up to a minute after the flash. The abolition of variable fluorescence in the strong WL pulse (Fig. 4*a*, *b*, *f*) and its near complete restoration within 2 s is comparable to that observed in the saturating pulse of PAM and gives values of $F_mWL \approx F_mPAM$ and $\phi_{PSII}WL \approx \phi_{PSII}PAM$ for estimating PAM equivalent NPQ and ETR. Although these dynamic changes render FRR model estimates of other parameters unreliable within the broken lines of Fig. 4, subsequent Q_A flash transients provide information about the kinetics of $Q_A \rightarrow$ PQ pool and PQ pool $\rightarrow$ PSI, electron transport, the relative PQ pool oxidation status, and σ_{PSII} and a_{PSII} as they relax back to the dark steady state.

Both F_mQ_A and F_o are stable in the dark before the WL pulse, confirming negligible effects of the cumulative excitation energy of the LIFT/FRR Q_A flash. The time-averaged excitation power during the continuous Q_A protocol is ~1.6 μm quanta m^{-2} s^{-1}, which appears to be sufficient to maintain the photosynthetic apparatus in a close-to dark adapted state. However, F_mQ_A increases by ~60% during the WL pulse, returning to the pre-flash level ~25 s after cessation of the pulse. Within 6 s after the flash $\phi_{PSII}Q_A$ returns to the pre-flash level, whereas F_mQ_A still exceeds the pre-flash level by 38%, indicating that the increase in F_mQ_A is not related to the level of Q_A reduction. A similar ~25 s response in the kinetics of PQ pool re-oxidation (Fig. 4*c*) supports the previously-expressed notion that the level of PQ pool reduction controls the rise of F_mQ_A above that attained upon near full reduction of Q_A.

The kinetic of F_oQ_A relaxation more closely reflects re-oxidation of Q_A after cessation of the WL pulse. Although $\phi_{PSII}Q_A$ returns to pre-flash level within 6 s, F_oQ_A still exceeds the pre-flash level by ~30%, indicating that the level of PQ pool reduction controls not only the F_m, but also F_o (the fluorescence yields with fully oxidised Q_A). Deceleration of the kinetics of RQ_A relaxation (Fig. 4*f*, *g*), indicating a transient slowing of ETR $Q_A \rightarrow$ PQ (Fig. 4*c*), is the most prominent of these responses and is attributable to the increase in PQ pool reduction induced by the WL pulse (Fig. 3). The τ_1 reported in Fig. 4*c* (~1 ms) represents the average time constants of the two-stage, $Q_A \rightarrow Q_B$, and $Q_B \rightarrow$ PQ pool electron transport. This value is close to a weighted average of corresponding time constants reported in Kolber *et al*. (1998). We note that τ_1 transiently increases to ~6 ms following the short exposure to the WL pulse, relaxing to the pre-exposure level with the next 60 s. We attribute this slowing to transient reduction of the PQ pool, and the resulting slowdown of the $Q_B \rightarrow$ PQ pool electron transport. Relatively slow rates of PQ pool $\rightarrow$ PSI electron transport reported in Fig. 4*e*, (~20 ms) are typical of dark adapted conditions. These rates generally increase by a factor of 3–4 under low-to moderate irradiance levels. The strong light WL pulse accelerates these rates 2-fold (τ_2 transiently decreases to ~10 ms) before recovering slowly to the pre-exposure level over the next 2–3 min.

Publisher: CSIRO; Journal: FP:Functional Plant Biology
Article Type: research-article; Volume: ; Issue: ; Article ID: FP17024
DOI: 10.1071/FP17024; TOC Head:

Our interpretation of RQ_A kinetics is not limited by experimental noise in these data from the prototype LIFT (Figs 1, 2, 4), but is governed by the quality of FRR models and corresponding numerical procedures. There is a danger of over-interpreting data using models with too many degrees of freedom. We use the more conservative, two-stage model of electron transport to minimise this problem (as compared with a more sophisticated, three-stage model described in http://soliense.com/LIFT_Method.php, accessed 10 May 2017). The values of τ_1 and τ_2 reported in Fig. 4*c*, *d* represent experimentally monitored rates of electron transport *in situ* that illustrate the amplitude and dynamics of these processes during plant responses to changing irradiance.

Functional absorption cross-section (Fig. 4*e*) shows a transient, ~15% decrease in σ_{PSII}, recovering to a pre-flash level with kinetics similar to PQ pool re-oxidation. Within 6 s after the WL flash the continuously measured values of $\phi_{PSII}Q_A$ return to constant pre-flash levels, justifying calculation of optical absorption cross-section as $a_{PSII} = \sigma_{PSII}/\phi_{PSII}$ during this period (Fig. 4*e*) and accounting for the ~15% decrease after the WL flash that recovers with kinetics similar to the PQ pool. These data illustrate the need for high time-resolution monitoring of this property, but also justify the common practice of allowing ~30 s between saturating pulses of PAM measurements to minimise cumulative effects of PQ pool reduction.

Referencing $\phi_{PSII}Q_A$ and $\phi'_{PSII}Q_A$ against $\phi_{PSII}PQ$ and $\phi'_{PSII}PQ$, as well as against $\phi_{PSII}PAM$ and $\phi'_{PSII}PAM$ to obtain PAM-equivalent estimates of ETR

Most past applications of LIFT/FRR have focused on remote measurements of ETR and NPQ using empirical on-the-leaf calibrations against PAM and/or gas exchange. It is impractical to apply the strong WL pulse (Fig. 4) at a distance, so adoption of the 'double flash' protocol (Fig. 2*a*, *b*) provides a convenient surrogate estimate of $\phi_{PSII}Q_A$ vs $\phi_{PSII}PQ$ ($\approx\phi_{PSII}PAM$). The validity of inter-calibration measurements of $\phi'_{PSII}Q_A$ and $\phi'_{PSII}PQ$ from the 'double flash' of LIFT/FRR, and of $\phi'_{PSII}PAM$ from MINI-PAM, is readily demonstrated during light response curve experiments with sun and shade grown spinach, sun grown cotton and shade grown avocado and rubber plants (Fig. 5). These measurements were performed on the same, uniformly illuminated leaves after masking the MINI-PAM leaf clip to minimise possible actinic interference from saturating pulses, and applying LIFT/FRR 'double flashes' to adjacent areas, offset by 30 s. Two to six data points were obtained at 60 s intervals at each actinic PFD in steps ranging up to 530 μmol photons m^{-2} s^{-1} with shade grown avocado, rubber plants and spinach, and up to 890 μmol photons m^{-2} s^{-1} for sun grown cotton and spinach.

The $\phi'_{PSII}PQ$ vs $\phi'_{PSII}Q_A$ relationship is linear ($R^2 = 0.97$), with a well-defined, species-independent offset of ~0.16 (Fig. 5*a*), indicating that PQ pool reduction adds to the fluorescence signal, independent of the level of Q_A reduction, consistent with the interpretation of the J-I-P transient (Fig. 3). The relationship between $\phi'_{PSII}PAM$ and $\phi'_{PSII}Q_A$ is less constrained ($R^2 = 0.83$) with offset of 0.26 and much lower slope (Fig. 5*b*), suggesting a greater contribution of a Q_A-independent component to

Publisher: CSIRO; Journal: FP:Functional Plant Biology
Article Type: research-article; Volume: ; Issue: ; Article ID: FP17024
DOI: 10.1071/FP17024; TOC Head:

total fluorescence yield under conditions of fully reduced PQ pool based on these two signals. Nevertheless, the relationship between $\phi'_{PSII}PAM$ and $\phi'_{PSII}PQ$ is highly linear, with 1 : 1 slope and R^2 = 0.95 (Fig. 5*c*), confirming that these two techniques provide equivalent estimates of photosynthetic efficiency with a fully reduced PQ pool.

Consequently, fast transient light events requiring high temporal resolution (such as sun flecks) may be continuously monitored with the Q_A flash, by correcting $\phi'_{PSII}Q_A$ from a regression equation to estimate $\phi'_{PSII}PAM$ and thereby derive PAM-equivalent estimates of ETR using accepted relationships (Genty *et al*. 1989). For example, using the regression equation in Fig. 5*a* to recalculate the expected $\phi'_{PSII}PQ$ from measured $\phi'_{PSII}Q_A$:

$$\phi'_{PSII}PQ = 0.936 \times \phi'_{PSII}Q_A + 0.157, \quad (1)$$

and because $\phi'_{PSII}PQ \approx \phi'_{PSII}PAM$, the PAM-equivalent ETR from the LIFT Q_A flash = (0.936 × $\phi'_{PSII}Q_A$ + 0.157) × PFD × 0.425 (assuming 85% of incident light is absorbed and shared equally by PSII and PSI). These recalculated data from the LIFT/FRR Q_A flash at a distance give virtually identical rates of ETR in sun-grown spinach and shade-grown rubber plants to those derived from direct PAM measurements (Fig. 5*d*).

The flexible protocols of LIFT/FRR can be tailored to suit a diversity of laboratory and field experiments. Fig. 6, for example, shows three screen captures from laboratory measurements targeting a sun-grown spinach leaf with an excitation protocol designed as a 24 h long series of Q_A flashes at 2 s intervals with a PQ flash periodically inserted at ~60 s intervals. Set up in normal fluorescent laboratory light (7 μmol photons m^{-2} s^{-1}), the transfer to darkness (indicated by the bar in Fig. 6*a*) has profound effects on the kinetics of the fluorescence signal following the PQ flash. This can be ascribed to presence of traces of near infrared (nIR) in the fluorescent room light which is evidently sufficient to pull electrons from the PQ pool to PSI, resulting in quick (~2 s) re-oxidation of PQ pool following the prolonged 470nm flash of the PQ protocol, which in the dark is manifest as much slower (~15 s) recovery of F_mQ_A, ϕ_{PSII} and σ_{PSII} to pre-PQ flash levels (Fig. 6*a*). On the other hand, a similar effect is observed in presence of weak (~2 μmol photons m^{-2} s^{-1}) of blue light, indicating that maintenance of residual electron flow may be sufficient to establish conditions for quick re-oxidation of PQ pool after the PQ flash (data not shown).

Despite the ~20 fold larger cumulative energy of the PQ flash compared with the Q_A flash, the much longer period (~60 s) between PQ flashes ensures this excitation protocol remains minimally intrusive in the dark (Fig. 6*b*). The stability of F_mQ_A and $\phi_{PSII}Q_A$ as well as F_mPQ and $\phi_{PSII}PQ$ data show no detectable actinic effect of 3600 Q_A flashes and 120 PQ flashes over a period of 2 h. The PQ flash applied at this frequency allows referencing of Q_A flash-based monitoring of F_m, F'_m, ϕ_{PSII}, ϕ'_{PSII} for PAM-equivalent estimation of ETR and NPQ with a time resolution of 2 s during the transient following an increase from 10 to 120 μmol photons m^{-2} s^{-1} (Fig. 6*c*).

Publisher: CSIRO; Journal: FP:Functional Plant Biology
Article Type: research-article; Volume: ; Issue: ; Article ID: FP17024
DOI: 10.1071/FP17024; TOC Head:

Referencing F'_mQ_A against F'_mPQ, F'_mWL and F'_mPAM to obtain PAM equivalent estimates of NPQ

Since Bilger and Björkman (1990), NPQ in all its complexity, has been estimated from the simple Stern-Volmer equation NPQ = $(F_m/F'_m) - 1$. We expect that LIFT/FRR estimates of NPQ based on the PQ flash (using F_mPQ and F'_mPQ fluorescence signals) to closely follow PAM-based estimates of NPQ. Indeed, a photosynthetic induction experiment from dark to 100 µmol photons m^{-2} s^{-1} actinic light, interrogating the very same spot on an avocado shade leaf with both the actinic light and the saturating pulse from MINI-PAM and the 'double flash' of LIFT/FRR (at 60 s intervals offset by 30 s to avoid interference) yielded very similar estimates of NPQ (Fig. 7*a*).

Unfortunately, such comparisons cannot be made directly under conditions of rapid changes of ambient irradiance. Sun flecks, for example, require continuous monitoring with temporal resolution of up to 1 Hz. Thus, as suggested above, PAM-comparable NPQ may be calculated by correcting the continuously monitored signal with near fully reduced Q_A (F'_mQ_A) with signals obtained with fully reduced PQ pool using PQ flashes interspersed at 60 s intervals to obtain F_mPQ and F'_mPQ, or F'_mWL as reference (e.g. Fig. 6) as follows:

$$F_mQ_A \text{ (corr)} = a_{PQ} + (b_{PQ} \times F_mQ_A), \text{ and } F'_mQ_A \text{ (corr)} = a_{PQ} + (b_{PQ} \times F'_mQ_A), \quad (2)$$

where a_{PQ} and b_{PQ} are linear regression coefficients of F'_mPQ against F'_mQ_A from LRCs (e.g. Fig. 7*b*). Therefore:

$$\text{PAM-equivalent NPQ} = b_{PQ} \times (F_mQ_A - F'_mQ_A)/(a_{PQ} + b_{PQ} \times F'_mQ_A), \quad (3)$$

or when a strong WL pulse is used to obtain the correlation between F_mQ_A or F'_mQ_A:

$$\text{PAM-equivalent NPQ} = b_{WL} \times (F_mQ_A - F'_mQ_A)/(a_{WL} + b_{WL} \times F'_mQ_A). \quad (4)$$

Fig. 7*b* shows a regression equation for F_mWL vs F_mQ_A obtained before and during a strong WL pulse in *Arabidopsis* parent wild-type *pgr5bkg* and its NPQ impaired *pgr5* mutant (absence of proton gradient regulation protein *pgr5*; Munekage *et al*. 2002). A regression equation from a LRC with avocado leaves is also given in Fig. 7*b*. The values of a_{WL} and b_{WL} are used to obtain PAM-equivalent estimates of NPQ from LIFT for comparison with MINI-PAM measurements of NPQ at 30 s intervals after transfer of the low light-grown genotypes (120 µmol photons m^{-2} s^{-1}) to 1000 µmol photons m^{-2} s^{-1} WL for 6 min. The MINI-PAM data obtained on individual leaves are compared with LIFT assays on rosettes of the same plants allowed to recover in growth irradiance for 4 days. At corresponding time points, NPQ induction monitored by F'_mQ_A and corrected by the regression equation are highly correlated (Fig. 7*c*).

More importantly, the faster resolution of early NPQ kinetics available from the Q_A flash of LIFT is potentially of interest, especially with respect to distinguishing component processes. The PAM-based kinetic of NPQ in the parent genotype *pgr5 bkg* do not differ much from those obtained with high-resolution LIFT data. In the *pgr5* mutant, however, the high-resolution LIFT data reveals a substantial initial NPQ transient (Fig. 7*d*) that cannot be resolved with PAM assays at 30 s intervals.

Publisher: CSIRO; Journal: FP:Functional Plant Biology
Article Type: research-article; Volume: ; Issue: ; Article ID: FP17024
DOI: 10.1071/FP17024; TOC Head:

Although the initial rates of NPQ engagement in these genotypes is similar, the subsequent overshoot and decline of NPQ in the *pgr* mutant may reflect impaired regulation of ΔpH and linear ETR in *pgr5* which retains a more reduced PQ pool despite acceleration of ETR PQ → PSI (Suorsa *et al*. 2012; CB Osmond, unpubl. data). The ability to resolve fast components of NPQ kinetics will become extremely important to investigation of the different components of NPQ, especially during sun flecks.

Continuous monitoring of photosynthetic parameters with LIFT/FRR protocols is much less intrusive than PAM

When applied repeatedly at 2 s intervals the Q_A flash depicted in Fig. 1*a* delivers an average of ~1.6 μmol photons m^{-2} s^{-1} of 470 nm light. This cumulative actinic load is somewhat greater than the pulse modulated 450 nm measuring beam deployed by Junior-PAM (Heinz Walz GmbH, 91 090). Thus, the first Q_A flash applied to a dark-adapted leaf generally yields slightly higher values of F_oQ_A and F_mQ_A than the next Q_A flash, but usually it is not accompanied by changes in $\phi_{PSII}Q_A$ (data not shown). This initial change is consistent with the notion of partial reduction of the PQ pool in the dark, which disappears within the first few Q_A flashes as the level of PQ pool reduction stabilises due to partial activation of PSI by the 470 nm light. Following this initial change (which is absent at levels of background room light above 1–2 μmol photons m^{-2} s^{-1}; c.f. Fig. 6*a*), FRR fitted photosynthetic parameters remain stable in the dark with Q_A flashes applied at rates of one flash every 2–3 s or four flashes averaged every 5–6 s.

When high time resolution measurements are required the relatively non-intrusive Q_A flashes of LIFT/FRR stand in marked contrast to the much more intrusive saturating WL pulse of PAM (Apostol *et al*. 2001). Fig. 8 compares the impact of four successive Q_A flashes (applied at 1 s intervals then averaged every 5 s) with saturating pulses from MINI-PAM (normal or minimal intensity for data acquisition) at 10 s intervals on adjacent areas of the same leaf of shade grown spinach plants pre-adapted to weak laboratory light (~2 μmol photons m^{-2} s^{-1}). This comparison reveals that monitoring with the Q_A flash has little impact on F_oQ_A, F_mQ_A (Fig. 8*a, c*) or $\phi_{PSII}Q_A$ (Fig. 8*b, d*). Monitoring with PAM at half the time resolution produces substantial declines in F_o, F_mPAM and $\phi_{PSII}PAM$ due to the cumulative actinic effect of the saturating pulses, even at the lowest settings of measuring beam and saturating pulse intensity. Whereas the saturating pulse of PAM limits the frequency of data acquisition to ~30 to 60 s (with monitoring-PAM for example), LIFT measurements are minimally intrusive at 10–20 times higher temporal resolution.

Further evidence of the effects of measurement protocols, this time with large, thin shade leaves of avocado plants grown indoors is reported in Table 2. In this experiment, LIFT/FRR fluorescence data acquired using the ‘double flashes’ protocol (Q_A + PQ flash, with ~25 times higher excitation energy than Q_A flash alone) are compared with those obtained with MINI-PAM. The LIFT and MINI-PAM assays were applied at 1 min. intervals to adjacent areas of the large leaf, with timing of the saturating

Publisher: CSIRO; Journal: FP:Functional Plant Biology
Article Type: research-article; Volume: ; Issue: ; Article ID: FP17024
DOI: 10.1071/FP17024; TOC Head:

PAM pulse and the LIFT 'double flash' offset by 30 s and all but the leaf disc area exposed to the saturating pulse of MINI-PAM masked to minimise cross interference of the flashes. Successive measurements were taken in the dark before and after continuous exposure to WL in a prolonged LRC, comprising exposures for 3–6 min ramping from 37 to 526, then 66 and 56 μmol photons m^{-2} s^{-1}. The cumulative effects of the 'double flash' of LIFT on $\phi_{PSII}Q_A$ and $\phi_{PSII}PQ$ before and after the LRC (1.6 and 2.9% respectively) are ~10 and five times smaller than the cumulative impact of the saturating pulses on $\phi_{PSII}PAM$ (Table 2).

Validation of LIFT/FRR measurements of σ_{PSII} *and* a_{PSII}: *estimation of relative antenna size from* σ_{PSII} *in wild type and mutants of* Arabidopsis *and barley*

The LIFT/FRR approach to measurement of σ_{PSII} (functional absorption cross-section of PSII) from the Q_A flash transient assumes this parameter has two principal components: excitation harvesting in the antenna of the PSII complex (i.e. the optical absorption cross-section) and the photochemical efficiency of light use in the PSII reaction centre. Following work by Highkin (1950), many naturally occurring antenna size mutants have been characterised in barley, rice (Terao and Katoh 1996) and other crops, and much more research has been invested in the creation of antenna mutants of *Arabidopsis* differing in size and sub unit pigment compositions. Thus comparisons between wild types and mutants with well-established lesions in PSII antenna size offer the prospect for biological validation of LIFT/FRR model estimates of σ_{PSII} from the relationship $\sigma_{PSII} = a_{PSII} \times \phi_{PSII}$ (Kolber *et al*. 1998). With little variation in steady-state $\phi_{PSII}Q_A$ *in situ*, estimates of σ_{PSII} are expected to represent differences in antenna size among genotypes, and the mutant genotypes assayed in Table 3 shows that this is the case. Moreover, the relative optical absorption cross-section of PSII (a_{PSII}) estimated from LIFT/FRR measurements of σ_{PSII} and ϕ_{PSII} *in situ* are comparable to *in vitro* estimates of relative antenna size of mutants and wild types (Table 3).

Only a small number of mutant genotypes has been assayed to date, but the antenna size relative to wild type ranges from a consistent ~80% in *asLhcb2–12* (Andersson *et al*. 2003) compared with *Col* over several successive batches of these plants to a much larger reduction of σ_{PSII} and a_{PSII} in *ch1–3 Lhcb5*, down to 23% of *Col* (c.f. ~35%, Kim *et al*. 2009). The widely studied *chlorina-f2* mutant of barley (Highkin 1950) has a smaller PSII antenna that is depleted in Lhcb1, Lhcb4, and Lhcb6, with reduced amounts of Lhcb2, Lhcb3 and Lhcb5 (Bossmann *et al*. 1997). Our LIFT-based measurements of σ_{PSII} and a_{PSII} are somewhat higher (~35 to 45% of wild type; Table 3) than estimates from *in vitro* methods (~20% of *Col*; Cleland and Melis 1987; Harrison *et al*. 1993). When grown from the same seed batches in a greenhouse for long days with lower natural and artificial light intensities at Forschungszentrum Jülich noticeably lower values for σ_{PSII} and a_{PSII} were obtained (Table 3). This response to low growth irradiance was unexpected. These assays were made with a commercially available LIFT/FRR instrument using a different Q_A flash protocol, yet differences between wild type and *chlorina-f2* were proportionally quite similar to those obtained with full sun greenhouse cultivation in Canberra using the prototype instrument. A much more extensive range of

Publisher: CSIRO; Journal: FP:Functional Plant Biology
Article Type: research-article; Volume: ; Issue: ; Article ID: FP17024
DOI: 10.1071/FP17024; TOC Head:

antenna mutants is now available (e.g. Goral *et al.* 2012) for closer examination using commercial LIFT/FRR instruments.

Effects of growth irradiance on LIFT/FRR-measured σ_{PSII} and a_{PSII}

It has long been known that acclimation to shade and sun is accompanied by manifold changes in the structure and function of photosynthetic apparatus, from the structure of thylakoid membranes to the architecture of leaves and canopies (Björkman *et al*. 1972; Chow and Anderson 1987; Matsubara *et al*. 2012). It is not surprising therefore that when *Arabidopsis Col* is transferred from growth chambers to full sunlight in the glasshouse, both σ_{PSII} and a_{PSII} decline by ~25% after 10 days (Table 4). Similarly, σ_{PSII} of shade grown spinach is ~25% larger than of sun plants (data not shown) and when sun plants are kept in weak fluorescent laboratory light (< 5 μmol photons m^{-2} s^{-1}) for 4 days both σ_{PSII} and a_{PSII} increase by ~13% (Table 4). Five *Arabidopsis* genotypes grown under ~60–80 μmol photons m^{-2} s^{-1} have 14 - 65% larger a_{PSII} than those grown at 120 μmol photons m^{-2} s^{-1} (Table 5).

These LIFT/FRR data are consistent with earlier observations by Malkin and Fork (1981), that photosynthetic unit size ranged from 220 to 540 Chl *a*/ RCII in six species of sun plants and from 630 to 940 in six shade species. The optical absorption cross-section, in units of $Å^2$/PSII centre, quantifies the PSII-specific rates of light absorption. According to Ley and Mauzerall (1982), the molecular Chl *a* absorption cross-section at 596 nm is 0.29 $Å^2$. Here we assume that the optical absorption cross-section of Chl *a* and Chl *b* is similar at 596 nm, and we assume that they increase by a factor of 1–2 for Chl *a*, and by a factor of 10 for Chl *b* at 475 nm. We also assume the average 3 : 1 ratio of Chl *a*/Chl *b*. The weighted average of the optical cross-section Chl *a*/*b* at 475 should then be in $0.94A^2$ to 1.16 A^2 range. Further assuming that ~30% of photosynthetic light utilisation is due to accessory pigments, the remainder of our measured absorption cross-section would be contributed by 200 to 520 Chl *a*/*b* molecules in 3 : 1 ratio, comparable with the range of estimates based on chlorophyll fluorescence emission from DCMU infiltrated sun and shade leaves (Malkin and Fork 1981).

Our data also confirm earlier evidence for substantial light acclimation capacity of antenna size components in land plants (Melis and Anderson 1983) and algae (Kolber *et al*. 1988), and are consistent with recent *in vitro* estimates of the decline in antenna size of *Arabidopsis* in response to increasing growth irradiance (Ballottari *et al*. 2007; Mishra *et al*. 2012; Kouřil *et al*. 2013). Clearly, continuously monitored, *in-situ* measurements of relative σ_{PSII} and a_{PSII} from LIFT have the potential to replace currently used spot measurements of DCMU infused tissues.

Capturing the dynamics of photosynthetic responses to sun flecks in situ *with the Q_A flash of LIFT/FRR*

It is noticeable that, despite successful high time resolution monitoring of photosynthetic gas exchange (~1 s) in simulated sun flecks (Kirschbaum and Pearcy 1988*a*; Pearcy 1990), chlorophyll fluorescence methods have not been applied widely in such studies, presumably because the

Publisher: CSIRO; Journal: FP:Functional Plant Biology
Article Type: research-article; Volume: ; Issue: ; Article ID: FP17024
DOI: 10.1071/FP17024; TOC Head:

saturating pulse of PAM is intrusive on the short time scales needed to track these events. With the exception of some field studies (Watling *et al*. 1997; Adams *et al*. 1999), PAM techniques have found little application to the monitoring of sun flecks *in situ*. Kirschbaum and Pearcy (1988*b*) demonstrated that O_2 evolution from a fully induced *Alocasia* leaf in 10 μmol photons m^{-2} s^{-1} peaked immediately (within the 1 s resolution of the assay system) following a step change to ~500 μmol photons m^{-2} s^{-1}, then declined over ~10 s as rate limiting CO_2 fixation slowly increased. The rapid downregulation of the light reactions implied by these observations is surely of fundamental importance to our understanding of the regulation of primary photosynthetic processes in the stochastic inner canopy light environment, especially in windy conditions. From the data in Fig. 9, it is clear that the prototype LIFT/FRR offers time resolutions that approach, but do not yet match, the time resolution attained by leaf gas exchange methods three decades earlier!.

Inner canopy leaves of mature ~10 m high avocado trees in an established orchard (Alstonville, NSW) experience frequent lower intensity natural canopy sun flecks that are readily tracked by the ULM light meter with a time resolution of 10 s. These leaves are also readily accessible for continuous monitoring with the Q_A flash of LIFT/FRR (4 successive Q_A flashes at ~1 Hz averaged at intervals of 5–6 s). This approach is illustrated by a brief (~3 min) morning sun fleck of moderate intensity (~250 μmol photons m^{-2} s^{-1}, Fig. 9). As in Fig. 4, selected data are colour-coded (Fig. 9*b*) to illustrate changes in the Q_A flash profiles (Fig. 9*f, g*), during three periods of interest, i.e. shown as (i), (ii) and (iii), separated by vertical lines in Fig. 9*a–e*.

With background diffuse canopy light (< 25 μmol photons m^{-2} s^{-1}) in (i) there is steady decline in $\phi'_{PSII}Q_A$ (Fig. 9*c*) due to an increase in $F'Q_A$ (Fig. 9*f*) followed by a weak canopy-filtered sun fleck that doubles PFD and ETR. The PQ pool becomes progressively more oxidised (Fig. 9*d*) and light use affinity increases (i.e. E_k declines; Fig. 9*e*). These changes are indicative of slow photosynthetic induction and adjustment to the diffuse low light environment and are accompanied by little overt change in shape of the Q_A flash profiles (Fig. 9*f*).

In period (ii) a marked departure of the co-dependence of ETR on PFD occurs when sun fleck exceeds PFD ~100 μmol photons m^{-2} s^{-1} (Fig. 9*a*). This is coincident with decline in F'_mQ_A and increase in $F'Q_A$ (open red, turquoise, purple and blue symbols; Fig. 9*b, g*). This decline in ETR relative to PFD indicates a decrease in light use efficiency; the ratio of photons/electron increases from 4.2 ± 0.1 in periods (i) and (iii) to 5.4 ± 0.2 during period (ii). This is accompanied by an increase in NPQ for ~60 s, concurrent with continued decline in $\phi'_{PSII}Q_A$ (Fig. 9*c*). We noted that E_k the simulated half saturation PFD for ETR follows $\phi'_{PSII}Q_A$ closely (Fig. 9*c, e*), both increasing strongly after NPQ stabilizes, then declining. The Q_A flash transients report the decline in F'_mQ_A (and then in $F'Q_A$) in the SQ_A phase and also show changes in RQ_A phases (c.f. Fig. 9*f, g*); indicating slowing of both ETR $Q_A \rightarrow$ PQ pool and PQ pool $\rightarrow$ PSI electron transport and further PQ pool

Publisher: CSIRO; Journal: FP:Functional Plant Biology
Article Type: research-article; Volume: ; Issue: ; Article ID: FP17024
DOI: 10.1071/FP17024; TOC Head:

oxidation (Fig. 9*d*). However there is no suggestion of RQ_A complexity associated with over-reduction of the PQ pool as seen in strong WL pulses (Fig. 4*f*, *g*).

The ETR vs PFD relationship is re-established within ~10 s when PFD drops from 274 to 100 µmol photons m^{-2} s^{-1} early in period (iii) and remains in step when PFD transiently increases again to ~240 µmol photons m^{-2} s^{-1} (blue, grey, red and open black symbols; Fig. 9*h*), as well as throughout the next sun fleck (~90 µmol photons m^{-2} s^{-1}). In contrast to period (ii), NPQ now declines rapidly and remains low thereafter, and E_k returns rapidly to background levels in diffuse light.

In general terms, both SQ_A and RQ_A components of Q_A flash profiles return to diffuse light format and respond as in (i). Changes in σ'_{PSII} and a'_{PSII} are small and oscillatory (Fig. 9*e*), and coordinated with small increases in PQ pool oxidation (Fig. 9*d*). Overall, this avocado shade leaf shows rapid, well co-ordinated responses to photosynthetic induction and rapidly reversible photoprotection during sun flecks. Clearly, the Q_A flash of LIFT/FRR is well suited for further exploration of these phenomena in fluctuating light, as well as and evaluation of long-term photosynthetic acclimation to sun and shade environments.

Discussion and conclusions

The techniques and data presented above comprehensively outline an approach to relatively non-intrusive, monitoring of chlorophyll fluorescence *in situ* in terrestrial environments using the Q_A flash of LIFT/FRR at a distance of 0.5–2.0 m with a temporal resolution of a few seconds. When fitted to the FRR model (Kolber *et al*. 1998) each Q_A flash transient provides values of intrinsic chlorophyll fluorescence yield (F_oQ_A), maximum yield (F_mQ_A), variable fluorescence (maximum photochemical efficiency of PSII, $\phi_{PSII}Q_A$). The nomenclature introduced in Table 1 mitigates ambiguities that arise during comparisons of fluorescence data from different LIFT/FRR assays and PAM by simply appending postfixes to traditionally used abbreviations. For example, the generally lower values of $\phi_{PSII}Q_A$ obtained by the Q_A flash of LIFT/FRR in the dark are distinguished from those monitored by the this protocol during a strong PAM analogous WL pulse as $\phi_{PSII}WL$, which are in turn equivalent to $\phi_{PSII}PAM$ obtained in the saturating pulse of PAM.

We propose that differences in these values arise because the ~0.5 ms Q_A flash measures PSII fluorescence yield with near fully reduced Q_A before electron transfer to PQ (i.e. during the 'photochemical' J phase of the O-J-I-P transient) whereas the additional PSII fluorescence yield measured by the >500 ms saturating pulse of PAM arises during the 'thermal' J-I-P phases of the O-J-I-P transient (Strasser *et al*. 1995). These differences disappear when ϕ_{PSII} is measured with the Q_A flash during a strong PAM analogous WL pulse and in the PQ flash from LIFT/FRR; i.e. $\phi_{PSII}WL \approx \phi_{PSII}PQ \approx \phi_{PSII}PAM$. Decades of immensely rich studies of O-J-I-P phenomena (Stirbet and Govindjee 2012; Schansker *et al*. 2014; Vredenberg 2015; Kalaji *et al*. 2017) have discussed many factors that may be responsible for the increase in fluorescence yield during progressive reduction of

Publisher: CSIRO; Journal: FP:Functional Plant Biology
Article Type: research-article; Volume: ; Issue: ; Article ID: FP17024
DOI: 10.1071/FP17024; TOC Head:

PQ pool. Perhaps the simplest and most verifiable is the occupancy of the Q_B site. As the level of PQ pool reduction increases, so does the fraction of unoccupied Q_B sites on D1 protein, possibly leading to an increase of the fluorescence signal above that attributable to reduced Q_A. This action is similar to that of DCMU, where the inhibitor molecule is lodged in the Q_B site, preventing quinone docking. As a result, Q_A^- re-oxidation time increases to 300–600 ms, whereas the F_mQ_A signal becomes comparable to F_mPQ signal (data not shown). One of the possible mechanisms for fluorescence rise under these conditions is the charge recombination between Q_A^- and the donor side of PSII (Goltsev *et al.* 2009; Strasser *et al.* 2010), although the large, 30–40% increase in the fluorescence signal cannot be explained solely by the relatively weak amplitude of the 'delayed' fluorescence.

Rapid modulation of the amplitude of LIFT/FRR fluorescence transient, above and beyond the level of Q_A reduction, may also involve the back-reaction between Q_A^-/Q_B^- and P680+. This is likely to come into play during longer excitation protocols, such as the LIFT PQ protocol, or the saturating pulse of PAM (Strasser *et al*. 2010). Intuitively, the much lower excitation energy of the LIFT PQ flash compared with PAM saturating pulse should make the PQ flash less susceptible to this effect. Nevertheless, as these assays produce $\phi_{PSII}PQ \approx \phi_{PSII}PAM$, we conclude, that within the range of experimental conditions employed here, the effects of the back reaction (if any) on these signals is either negligible, or similar.

In the field it is impractical to deliver saturating WL pulses at a distance, but we show that the Q_A flash and PQ flash from the 'double flash' of LIFT/FRR yields reliable surrogate values of F_mPQ and $\phi_{PSII}PQ$ for cross calibration with the Q_A flash, providing regression equations for PAM-equivalent estimates of NPQ and ETR from Q_A flash data in traditional induction and light response curves with a time resolution of up to ~2s. Also, if a PQ flash is inserted at 60 s intervals into a continuous train of Q_A flashes, the average excitation pressure is reduced to a level that allows non-intrusive measurements of ETR and NPQ at intervals of a few seconds between PQ flashes over periods of hours (Fig. 6). In general terms, this combination of LIFT/FRR protocols is ~20 fold less intrusive than PAM when applied with ~20 fold higher time resolution.

Apart from minimally intrusive, high time resolution observation of chlorophyll fluorescence parameters at a distance, the principal contribution of the LIFT/FRR Q_A flash may be that it provides direct access to PSII primary processes *in situ* with minimal perturbation arising from the redox state of the PQ pool. Estimates of the relative functional (σ_{PSII}) and optical (a_{PSII}) absorption cross-sections of PSII are dominated by the initial SQ_A phase of the Q_A flash, but the whole transient is fitted by the FRR model. These estimates require knowledge of the incident excitation power and light attenuation across the leaf tissue but it is difficult to estimate the excitation power below the first layer of the leaf cells. The heterogeneous morphology of the leaf tissue (e.g. Terashima and Inoue 1984; Oguchi *et al.* 2005), further complicates the task of absolute assessments of σ_{PSII}. Even if we could reconstruct the light field below this layer (e.g. by adapting the PROSPECT model; Jacquemoud *et al*. 1996)

Publisher: CSIRO; Journal: FP:Functional Plant Biology
Article Type: research-article; Volume: ; Issue: ; Article ID: FP17024
DOI: 10.1071/FP17024; TOC Head:

accounting for the heterogeneous light field presents numerical problems in data analysis that (at least for now) are beyond our capabilities. To date, the efficacy of these approaches for improving the accuracy of σ_{PSII} estimates has not been rigorously investigated.

While acknowledging that estimates of σ_{PSII} are strictly only valid in dilute suspensions/thin samples, Klughammer and Schreiber (2015) also point out, 'some of these parameters reflect intrinsic properties of PSII, and hence, can be assumed to be independent of cell density'. Furthermore, they indicate that 'the apparent wavelength dependent absorption cross-sections of PSII in optically dense suspensions are closely related to the effective PAR'. Likewise, our immediate objective is to use relative changes in σ_{PSII} as a measure of sunlight utilisation by the leaf as a whole. In this context, the heterogeneity of the light field, and the heterogeneity of the of the σ_{PSII} across the leaf tissue as observed and averaged by the LIFT instrument should be similar to that experienced and averaged by the leaf in response to sunlight.

Our biological validation of σ_{PSII} and a_{PSII} in dark adapted antenna size mutants and wild types grown in sun and shade environments gives us confidence that despite all of the potential shortcomings, the LIFT/FRR approach is sufficiently accurate to quantify differences in these parameters. Estimates of relative σ_{PSII} (and a_{PSII}) *in situ* are proportionally similar to literature estimates from destructive *in vitro* analyses and to estimates of PSII unit size obtained from fluorescence induction experiments with DCMU treated leaves. There is room for much further confirmation of these relationships with other genotypes and mutants. Specifically, the conclusion of Ware *et al*. (2015) that 'not only the total antenna size, but also the functional cross-section varies with acclimation, increasing under lower light intensities' is now verifiable and quantifiable *in situ* under a wide range of conditions.

Additionally, we observe systematic highly dynamic responses of σ_{PSII} to ~1 s exposure to strong light (Fig. 4*e*), where the potential effects of back-reactions before, and after the flash, are likely to be similar. Although we cannot exclude the potential effects of back-reactions on LIFT/FRR-derived σ_{PSII} these effects are unlikely to invalidate our observations. The ~14% decline in σ_{PSII} and a_{PSII} within 15 s following a strong WL pulse and their recovery after ~30 s tracks the recovery of F_mQ_A, F_o and the PQ pool oxidation level. An order of magnitude faster than classical NPQ, these processes may be involved in the subsecond downregulation of the burst in O_2 evolution *in situ*, that mirrors the slower induction of CO_2 fixation in *Alocasia* (Kirschbaum and Pearcy 1988*b*) and pumpkin (Laisk and Oja 1998) leaves following sudden increases in PFD. These parameters also respond quickly to very low intensities of nFR light, indicating close functional relationships between redox state of the PQ pool, σ_{PSII} and a_{PSII} that invite close evaluation of their ability to monitor the conditions responsible for driving state transitions *in situ*.

This potential is clearly illustrated by observations on avocado shade canopy leaves during natural sun flecks (Fig. 9). Photosynthetic induction in weak diffuse shade light, with low rates of ETR

Publisher: CSIRO; Journal: FP:Functional Plant Biology
Article Type: research-article; Volume: ; Issue: ; Article ID: FP17024
DOI: 10.1071/FP17024; TOC Head:

characterised by a slow increase in affinity of light use (decline in E_k) and in PQ pool oxidation is interrupted by a sun fleck that accelerates ETR and increases the low level NPQ by 50% over ~60 s. As PFD exceeds ~100 μmol photons m^{-2} s^{-1} the efficiency of light use declines by ~25% but as the sun fleck passes and PFD drops below 100 μmol photons m^{-2} s^{-1} for ~10 s, NPQ relaxes and light use efficiency of ~4 photons $electron^{-1}$ is restored and persists throughout subsequent equivalent (and smaller) sun flecks.

These rapid and reversible changes in NPQ are only observed when the first sun fleck exceeds ~100 μmol photons m^{-2} s^{-1}. They are unlikely to involve de-epoxidation of xanthophyll pigments as little de-epoxidation of Lx or V occurs during 90 min. exposure of avocado shade leaves to 80 μmol photons m^{-2} s^{-1} sunlight (Förster *et al*. 2011). The old avocado shade leaf assayed here, and other avocado leaves sampled in similar canopy environments contain similar background concentrations (25–35 μmol mol^{-1} chl) of violaxanthin (V) and lutein epoxide (Lx) with persistent antheraxanthin (A, ~15 μmol mol^{-1} chl) and only traces of zeaxanthin (Z). High [Lx] is thought to promote efficiency of light capture in weak light (Matsubara *et al*. 2007) and this may explain high efficiency of ETR in diffuse deep canopy shade (~25 μmol photons m^{-2} s^{-1}; periods (i) and (iii) in Fig. 9*a*. Moreover, high residual Lx and A may promote rapidly reversible ΔpH-dependent NPQ in these plants (Matsubara *et al*. 2011) and this may be the source of the NPQ during the first sun fleck that is lost within seconds when PFD drops below this threshold. In these brief, relatively weak sun flecks ϕ'_{PSII} and E_k return to diffuse light levels and there is little perturbation of σ'_{PSII}, a'_{PSII} and ETR $Q_A \rightarrow$ PQ and PQ $\rightarrow$ PSI. Does this indicate intricately coordinated induction of photosynthesis in the shade?

In general, at this stage of enquiry, we believe the ability to observe the dynamics of these parameters *in situ*, in relative terms, following stochastic variations in the intensity and spectral composition of light environments under natural conditions is potentially more valuable than pursuit of absolute values of individual parameters obtained *in vitro*. Observations on the component responses of the 'holistic signature of photosynthetic parameters' available from the Q_A flash of LIFT/FRR to rapidly-varying irradiance regimes in the laboratory and in the natural environment, seem likely to reveal a range of regulatory mechanisms that may provide insights to integration of photosynthetic processes *in situ*.

In conclusion, the observations reported here encourage field-based applications of LIFT/FRR approach to monitor the dynamics of an expanded array of photosynthetic parameters *in situ*, beyond its contribution minimally intrusive, high time resolution assays of ETR and NPQ. The potential for deeper mechanistic insights into the light reactions of photosynthesis during highly stochastic inner canopy light environments under field conditions (Pearcy and Way 2012; Smith and Berry 2013) is substantial. Ideally, these capabilities now need to accompany rapid-response CO_2 and O_2 gas exchange systems. These have been available for decades (Kirschbaum and Pearcy 1988*b*; Laisk and

Publisher: CSIRO; Journal: FP:Functional Plant Biology
Article Type: research-article; Volume: ; Issue: ; Article ID: FP17024
DOI: 10.1071/FP17024; TOC Head:

Oja 1998) with time resolutions faster than the Q_A flash used here, but are not yet available for field use. Subsequent reports will deal with monitoring of state transitions and NPQ under contrived laboratory conditions using the prototype described here, and further evaluations of naturally occurring sun flecks in canopies of mature avocado trees in the field.

Acknowledgements

This research was initiated by a University of Wollongong start-up grant that facilitated the development of the LIFT instrument by Zbigniew Kolber who also advised on its set up. Australian Research Council grants DP120100872 (to the late Warwick Hillier) supported WSC and AZ, DP140101488 supported SAR and RW is in receipt of a Research Training Program scholarship. The O-J-I-P data were obtained with a M-PEA instrument kindly made available by Professor Reto Strasser, Bioenergetics Laboratory, University of Geneva, Jussy/Geneva Switzerland. Seed of *stn7*, *stn7/8*, *pgr5 bkg*, *pgr5* were provided by Eva-Mari Aro and Marjaana Suorsa, Department of Biochemistry, Molecular Plant Biology, University of Turku Finland. Agu Laisk, Tartu Ülikooli Tehnoloogiainstituut, Tartu, Estonia identified many opportunities for improvement in a previous manuscript. We thank Derek Collinge for germination and maintenance of *Arabidopsis* genotypes in the laboratory of BJP, and are grateful to Steve Dempsey and Gavin Pritchard for the glasshouse cultivation of the other plants used. This paper is dedicated to the memory of our esteemed colleague Jan Anderson for her encouragement throughout many of the issues explored here.

References

<jrn>Adams WW, III, Demmig-Adams B, Logan BA, Barker DH, Osmond CB (1999) Rapid change in xanthophyll cycle-dependent energy dissipation and photosystem II efficiency in two vines: *Stephania japonica* and *Smilax australis*, growing in the understorey of an open Eucalyptus forest. *Plant, Cell & Environment* **22**, 125–136. doi:10.1046/j.1365-3040.1999.00369.x</jrn>

<jrn>Ananyev G, Kolber ZS, Klimov D, Falkowski PG, Berry JA, Rascher U, Martin R, Osmond B (2005) Remote sensing of heterogeneity in photosynthetic efficiency, electron transport and dissipation of excess light in *Populus deltoides* stands under ambient and elevated CO_2 concentrations, and in a tropical forest canopy, using a new laser-induced fluorescence transient (LIFT) device. *Global Change Biology* **11**, 1195–1206. doi:10.1111/j.1365-2486.2005.00988.x</jrn>

<jrn>Andersson J, Wentworth M, Walters RG, Howard CA, Ruban AV, Horton P, Jansson S (2003) Absence of the Lhcb1 and Lhcb2 proteins of the light-harvesting complex of photosystem II – effects on photosynthesis, grana stacking and fitness. *The Plant Journal* **35**, 350–361. doi:10.1046/j.1365-313X.2003.01811.x</jrn>

<jrn>Apostol S, Briantais JM, Moise N, Cerovic Z, Moya I (2001) Photoinactivation of the photosynthetic electron transport chain by accumulation of over-saturating light pulses given to dark adapted pea leaves. *Photosynthesis Research* **67**, 215–227. doi:10.1023/A:1010676618028</jrn>

<jrn>Baker NR (2008) Chlorophyll fluorescence: a probe of photosynthesis in vivo. *Annual Review of Plant Biology* **59**, 89–113. doi:10.1146/annurev.arplant.59.032607.092759</jrn>

<jrn>Ballottari M, Dall'Osto L, Morosinotto T, Bassi R (2007) Contrasting behaviour of higher plant photosystem I and II antenna systems during acclimation. *The Journal of Biological Chemistry* **282**, 8947–8958. doi:10.1074/jbc.M606417200</jrn>

Belgio E, Kapitonova E, Chemliov J, Duffy, CDP, Ungerer P, Valkunasw L, Ruban AV (2014) Economic photoprotection in photosystem II that retains a complete light-harvesting system with slow energy traps. *Nature communications* **5**, 4433. doi: 10.1038/ncomms5433

<jrn>Bilger W, Björkman O (1990) Role of the xanthophyll cycle in photoprotection elucidated by measurements of light-induced absorbance changes fluorescence and photosynthesis in leaves of *Hedra canariensis*. *Photosynthesis Research* **25**, 173–185. doi:10.1007/BF00033159</jrn>

<jrn>Björkman O, Boardman NK, Anderson JM, Thorne SW, Goodchild DJ, Pyliotis NA (1972) Effect of light intensity during growth of *Atriplex patula* on the capacity of photosynthetic reactions, chloroplast components and structure. *Carnegie Institution of Washington Year Book* **71**, 115–135.</jrn>

<jrn>Bonardi V, Pesaresi P, Becker T, Schleiff E, Wagner R, Pfannschmidt T, Jahns P, Leister D (2005) Photosystem II core phosphorylation and photosynthetic acclimation require two different protein kinases. *Nature* **437**, 1179–1182. doi:10.1038/nature04016</jrn>

<jrn>Bossmann B, Knoetzel J, Jansson S (1997) Screening *chlorina* mutants of barley (*H. vulgare* L.) with antibodies against light-harvesting proteins of PSI and PSII: absence of specific antenna proteins. *Photosynthesis Research* **52**, 127–136. doi:10.1023/A:1005823711838</jrn>

<jrn>Bradbury M, Baker NR (1981) Analysis of the slow phase of the *in vivo* chlorophyll fluorescence induction curve. Changes in the redox state of photosystem II electron acceptors and fluorescence emission from photosystem I. *Biochimica et Biophysica Acta* **635**, 542–551. doi:10.1016/0005-2728(81)90113-4</jrn>

<jrn>Briantais J-M, Vernotte C, Picaud M, Krause GH (1979) A quantitative study of the slow decline of chlorophyll *a* fluorescence in isolated chloroplasts. *Biochimica et Biophysica Acta* **548**, 128–138. doi:10.1016/0005-2728(79)90193-2</jrn>

<jrn>Cerovic ZG, Goulas Y, Gorbunov M, Briantais J-M, Camenen L, Moya I (1996) Fluorosensing of water stress in plants; yield of chlorophyll fluorescence measured simultaneously and at a distance with a τ-LIDAR and a modified PAM-fluorimeter in maize, sugar-beet and Kalanchoe. *Remote Sensing of Environment* **58**, 311–321. doi:10.1016/S0034-4257(96)00076-4</jrn>

<jrn>Chappelle EW, Wood FM, Jr, McMurtrey JE, III, Newcomb WW (1984) Laser-induced fluorescence of green plants. 1: A technique for the remote detection of plant stress and species differentiation. *Applied Optics* **23**, 134–138. doi:10.1364/AO.23.000134</jrn>

<jrn>Chow WS, Anderson JM (1987) Photosynthetic responses of *Pisum sativum* to an increase in irradiance in growth I. Photosynthetic activities. *Australian Journal of Plant Physiology* **14**, 1–8. doi:10.1071/PP9870001</jrn>

Publisher: CSIRO; Journal: FP:Functional Plant Biology
Article Type: research-article; Volume: ; Issue: ; Article ID: FP17024
DOI: 10.1071/FP17024; TOC Head:

<jrn>Cleland RE, Melis A (1987) Probing the events of photoinhibition by altering electron-transport activity and light-harvesting capacity in chloroplast thylakoids. *Plant, Cell & Environment* **10**, 747–752.</jrn>

<edb>Duysens LNM, Sweers HE (1963) Mechanisms of two photochemical reactions in algae as studied by means of fluorescence. In 'Studies on microalgae and photosynthetic bacteria'. (Eds Japanese Society of Plant Physiologists) pp. 353–372. (University of Tokyo Press: Tokyo)</edb>

<jrn>Falkowski PG, Kolber Z (1995) Variations in chlorophyll fluorescence yields in phytoplankton in world oceans. *Australian Journal of Plant Physiology* **22**, 341–355. doi:10.1071/PP9950341</jrn>

<jrn>Flexas J, Briantis J-M, Cerovic Z, Medrano H, Moya I (2000) Steady-state and maximum chlorophyll fluorescence responses to water stress in grapevine leaves: a new remote sensing system. *Remote Sensing of Environment* **73**, 283–297. doi:10.1016/S0034-4257(00)00104-8</jrn>

<jrn>Förster B, Osmond CB, Pogson BJ (2011) Lutein from de-epoxidation of lutein epoxide replaces zeaxanthin to sustain enhanced capacity for non-photochemical chlorophyll fluorescence quenching in avocado shade leaves in the dark. *Plant Physiology* **156**, 393–403. doi:10.1104/pp.111.173369</jrn>

<jrn>Genty B, Briantais J-M, Baker NR (1989) The relationship between the quantum yield of photosynthetic electron transport and quenching of chlorophyll fluorescence. *Biochimica et Biophysica Acta* **990**, 87–92. doi:10.1016/S0304-4165(89)80016-9</jrn>

<jrn>Goltsev V, Zaharieva I, Chernev P, Strasser RJ (2009) Delayed fluorescence in photosynthesis. *Photosynthesis Research* **101**, 217–232. doi:10.1007/s11120-009-9451-1</jrn>

<jrn>Goral TK, Johnson MP, Duffy CDP, Brain APR, Ruban AV, Mullineaux CP (2012) Light harvesting antenna composition controls the macrostructure and dynamics of thylakoid membranes in *Arabidopsis*. *The Plant Journal* **69**, 289–301. doi:10.1111/j.1365-313X.2011.04790.x</jrn>

<jrn>Gorbunov MY, Kolber ZS, Falkowski PG (2000) Measurement of photosynthetic parameters in benthic organisms *in situ* using a SCUBA-based fast repetition rate fluorometer. *Limnology and Oceanography* **45**, 242–245. doi:10.4319/lo.2000.45.1.0242</jrn>

<jrn>Govindjee (1995) Sixty three years since Kautsky. *Australian Journal of Plant Physiology* **22**, 131–160. doi:10.1071/PP9950131</jrn>

<jrn>Harrison MA, Nemson JA, Melis A (1993) Assembly and composition of the chlorophyll *a*-*b* light-harvesting complex of barley (*Hordeum vulgare* L.): Immunochemical analysis of chlorophyll *b*-less and chlorophyll *b*-deficient mutants. *Photosynthesis Research* **38**, 141–151. doi:10.1007/BF00146413</jrn>

<jrn>Highkin HR (1950) Chlorophyll studies on barley mutants. *Plant Physiology* **25**, 294–306. doi:10.1104/pp.25.2.294</jrn>

<jrn>Jacquemoud S, Ustin SL, Verdebout J, Schmuk G, Andreoli G, Hosgood B (1996) Estimating leaf biochemistry using the PROSPECT leaf optical properties model. *Remote Sensing of Environment* **56**, 194–202. doi:10.1016/0034-4257(95)00238-3</jrn>

<jrn>Jia HS, Förster B, Chow WS, Pogson BJ, Osmond CB (2013) Decreased photochemical efficiency of photosystem II following sunlight exposure of shade-grown leaves of avocado (*Persea americana* Mill.):

because of, or in spite of, two kinetically distinct xanthophyll cycles? *Plant Physiology* **161**, 836–852. doi:10.1104/pp.112.209692</jrn>

<jrn>Kalaji HM, Schansker G, Brestic M, Bussotti F, Calatayud A, Ferroni L, Goltsev V, Guidi L, Jajoo A, Li P, *et al.* (2017) Frequently asked questions about fluorescence, the sequel. *Photosynthesis Research* **132**, 13–66. doi:10.1007/s11120-016-0318-y</jrn>

<jrn>Kautsky H, Hirsch A (1931) Neue Versuche zur Kohlensäureassimilation. *Naturwissenschaften* **19**, 964. doi:10.1007/BF01516164</jrn>

<jrn>Kim E-H, Li X-P, Razeghifard R, Anderson JM, Niyogi KK, Pogson BJ, Chow WS (2009) The multiple roles of light-harvesting chlorophyll *a*/*b*-protein complexes define structure and optimize function of *Arabidopsis* chloroplasts: a study using two chlorophyll *b*-less mutants. *Biochimica et Biophysica Acta* **1787**, 973–984. doi:10.1016/j.bbabio.2009.04.009</jrn>

<jrn>Kirschbaum MUF, Pearcy RW (1988*a*) Gas exchange analysis of the relative importance of stomatal and biochemical factors in photosynthetic induction in *Alocasia macrorrhiza*. *Plant Physiology* **86**, 782–785. doi:10.1104/pp.86.3.782</jrn>

<jrn>Kirschbaum MUF, Pearcy RW (1988*b*) Concurrent measurements of O_2 and CO_2 exchange during lightflecks in *Alocasia macrorrhiza* (L.) G. Don. *Planta* **174**, 527–533. doi:10.1007/BF00634483</jrn>

<jrn>Klughammer C, Schreiber U (2015) Apparent PS II absorption cross-section and estimation of mean PAR in optically thin and dense suspensions of *Chlorella*. *Photosynthesis Research* **123**, 77–92. doi:10.1007/s11120-014-0040-6</jrn>

<jrn>Kolber ZS, Falkowski PG (1993) Use of active fluorescence to estimate phytoplankton photosynthesis in situ. *Limnology and Oceanography* **38**, 1646–1665. doi:10.4319/lo.1993.38.8.1646</jrn>

<jrn>Kolber Z, Zehr J, Falkowski PG (1988) Effects of growth irradiance and nitrogen limitation on photosynthetic energy conservation in photosystem II. *Plant Physiology* **88**, 923–929. doi:10.1104/pp.88.3.923</jrn>

<jrn>Kolber Z, Prasil O, Falkowski PG (1998) Measurements of variable chlorophyll fluorescence using fast repetition rate techniques: defining methodology and experimental protocols. *Biochimica et Biophysica Acta - Bioenergetics* **1367**, 88–106. doi:10.1016/S0005-2728(98)00135-2</jrn>

<jrn>Kolber Z, Klimov D, Ananyev G, Rascher U, Berry J, Osmond B (2005) Measuring photosynthetic parameters at a distance: laser induced fluorescence transient (LIFT) method for remote measurements of PSII in terrestrial vegetation. *Photosynthesis Research* **84**, 121–129. doi:10.1007/s11120-005-5092-1</jrn>

<jrn>Kouřil R, Wientjes E, Bultema JB, Croce R, Boekema EJ (2013) High-light vs. low-light acclimation on photosystem II composition and organization in *Arabidopsis thaliana*. *Biochimica et Biophysica Acta* **1827**, 411–419. doi:10.1016/j.bbabio.2012.12.003</jrn>

<jrn>Krause GH, Weis E (1991) Chlorophyll fluorescence and photosynthesis: the basics. *Annual Review of Plant Physiology and Plant Molecular Biology* **42**, 313–349. doi:10.1146/annurev.pp.42.060191.001525</jrn>

<bok>Laisk A, Oja V (1998) *Dynamics of leaf photosynthesis: rapid-response measurements and their interpretation*. CSIRO Publishing: Melbourne)</bok>

<edb>Lavorel J, Etienne A-L (1977) In vivo chlorophyll fluorescence. In 'Primary processes in photosynthesis'. (Ed. J Barber) pp. 203–268. (Elsevier/North Holland Biomedical Press: Amsterdam)</edb>

<jrn>Leigh LS, Burgess T, Marino DVB, Wei YD (1999) Tropical forest biome of Biosphere 2: structure, composition and results of the first 2 years of operation. *Ecological Engineering* **13**, 65–93. doi:10.1016/S0925-8574(98)00092-5</jrn>

<jrn>Ley AC, Mauzerall D (1982) Absolute absorption cross sections for photosystem II and the minimum quantum requirement for photosynthesis in *Chlorella vulgaris*. *Biochimica et Biophysica Acta* **680**, 95–106. doi:10.1016/0005-2728(82)90320-6</jrn>

<jrn>Li X-P, Müller-Moulé P, Gilmore AM, Niyogi KK (2002) PsbS-dependent enhancement of feedback de-excitation protects photosystem II from photoinhibition. *Proceedings of the National Academy of Sciences of the United States of America* **99**, 15222–15227. doi:10.1073/pnas.232447699</jrn>

<jrn>MacAlister EC, Myers J (1940) The time course of photosynthesis and fluorescence measured simultaneously. *Smithsonian Institution Miscellaneous Collection* **99**(6), 1–37.</jrn>

<jrn>Malkin S, Fork DC (1981) Photosynthetic units of sun and shade plants. *Plant Physiology* **67**, 580–583. doi:10.1104/pp.67.3.580</jrn>

<jrn>Matsubara S, Morosinotto T, Osmond CB, Bassi R (2007) Short- and long-term operation of the lutein-epoxide cycle in light-harvesting antenna complexes. *Plant Physiology* **144**, 926–941. doi:10.1104/pp.107.099077</jrn>

<jrn>Matsubara S, Chen Y-C, Caliandro R, Govindjee, Clegg RM (2011) Photosystem II fluorescence lifetime imaging in avocado leaves: contributions of the lutein epoxide and violaxanthin cycles to fluorescence quenching. *Journal of Photochemistry and Photobiology. B, Biology* **104**, 271–284. doi:10.1016/j.jphotobiol.2011.01.003</jrn>

<jrn>Matsubara S, Förster B, Waterman M, Robinson SA, Pogson BJ, Gunning B, Osmond B (2012) From ecophysiology to phenomics: some implications of photoprotection and shade-sun acclimation *in situ* for dynamics of thylakoids *in vitro*. *Philosophical Transactions of the Royal Society of London. Series B, Biological Sciences* **367**, 3503–3514. doi:10.1098/rstb.2012.0072</jrn>

<jrn>Maxwell K, Johnson GN (2000) Chlorophyll fluorescence – a practical guide. *Journal of Experimental Botany* **51**, 659–668.</jrn>

<jrn>Melis A, Anderson JM (1983) Structural and functional organization of the photosystems in spinach chloroplasts. Antenna size, relative electron-transport capacity and chlorophyll composition. *Biochimica et Biophysica Acta* **724**, 473–484. doi:10.1016/0005-2728(83)90108-1</jrn>

<jrn>Melrose DC, Oviatt CA, O'Reilly JE, Berman MS (2006) Comparisons of fast repetition rate fluorescence estimated primary production and ^{14}C uptake by phytoplankton. *Marine Ecology Progress Series* **311**, 37–46. doi:10.3354/meps311037</jrn>

<jrn>Mishra Y, Jänkänpää HJ, Kiss AZ, Funk C, Schröeder WP Jansson S (2012) *Arabidopsis* plants grown in the field and climate chambers differ significantly in leaf morphology and photosystem components. *BMC Plant Biology* **12**, 6. doi:10.1186/1471-2229-12-6</jrn>

<jrn>Munekage Y, Hojo M, Meurer J, Endo T, Tasaka M, Shikanai T (2002) PGR5 is involved in cyclic electron flow around photosystem I and is essential for photoprotection in *Arabidopsis*. *Cell* **110**, 361–371. doi:10.1016/S0092-8674(02)00867-X</jrn>

<jrn>Nichol CJ, Pieruschka R, Takayama K, Förster B, Kolber Z, Rascher U, Grace J, Robinson SA, Pogson B, Osmond B (2012) Canopy conundrums: building on the Biosphere 2 experience to scale measurements of inner and outer canopy photoprotection from the leaf to the landscape. *Functional Plant Biology* **39**, 1–24. doi:10.1071/FP11255</jrn>

<jrn>Niyogi KK, Grossman AR, Björkman O (1998) *Arabidopsis* mutants define a central role for the xanthophyll cycle in regulation of photosynthetic energy conversion. *The Plant Cell* **10**, 1121–1134. doi:10.1105/tpc.10.7.1121</jrn>

<jrn>Oguchi R, Hikosaka K, Hirose T (2005) Leaf anatomy as a constraint for photosynthetic acclimation: differential responses in leaf anatomy to increasing growth irradiance among three deciduous species. *Plant, Cell & Environment* **28**, 916–927. doi:10.1111/j.1365-3040.2005.01344.x</jrn>

<jrn>Ounis A, Evian S, Flexas J, Tosti S, Moya A (2001) Adaptation of a PAM-fluorometer for remote sensing of chlorophyll fluorescence. *Photosynthesis Research* **68**, 113–120. doi:10.1023/A:1011843131298</jrn>

<jrn>Oxborough K, Moore CM, Suggett DJ, Lawson T, Chan HG, Geider RJ (2012) Direct estimation of functional PSII reaction centre concentration and PSII electron flux on a volume basis: a new approach to the analysis of fast repetition rate fluorometry (FRR) data. *Limnology and Oceanography, Methods* **10**, 142–154. doi:10.4319/lom.2012.10.142</jrn>

<jrn>Papageorgiou G, Govindjee (1968) Light-induced changes in the fluorescence yield of chlorophyll *a* in vivo. II *Chlorella pyrenoidosa*. *Biophysical Journal* **8**, 1316–1328. doi:10.1016/S0006-3495(68)86558-0</jrn>

<jrn>Pearcy RW (1990) Sunflecks and photosynthesis in plant canopies. *Annual Review of Plant Physiology and Plant Molecular Biology* **41**, 421–453. doi:10.1146/annurev.pp.41.060190.002225</jrn>

<jrn>Pearcy RW, Way DA (2012) Two decades of sunfleck research: looking back to move forward. *Tree Physiology* **32**, 1059–1061. doi:10.1093/treephys/tps084</jrn>

<jrn>Pieruschka R, Klimov D, Kolber ZS, Berry JA (2010) Monitoring of cold and light stress impact on photosynthesis by using the laser induced fluorescence transient (LIFT) approach. *Functional Plant Biology* **37**, 395–402. doi:10.1071/FP09266</jrn>

<jrn>Pieruschka R, Albrecht H, Muller O, Berry JA, Klimov D, Kolber ZS, Malenovsky Z, Rascher U (2014) Daily and seasonal dynamics of remotely sensed photosynthetic efficiency in tree canopies. *Tree Physiology* **34**, 674–685. doi:10.1093/treephys/tpu035</jrn>

Publisher: CSIRO; Journal: FP:Functional Plant Biology
Article Type: research-article; Volume: ; Issue: ; Article ID: FP17024
DOI: 10.1071/FP17024; TOC Head:

<jrn>Porcar-Castell A, Pfündel E, Korhonen JFJ, Juurola E (2008) A new monitoring PAM fluorometer (MONI-PAM) to study the short-and long-term acclimation of photosystem II in field conditions. *Photosynthesis Research* **96**, 173–179. doi:10.1007/s11120-008-9292-3</jrn>

<jrn>Rascher U, Bobich EG, Lin G-H, Walter A, Morris T, Naumann M, Nichol CJ, Pierce D, Bil K, Kudeyarov V, Berry JA (2004) Functional diversity of photosynthesis during drought in model tropical rainforest – the contributions of leaf area, photosynthetic electron transport and stomatal conductance to reduction in net ecosystem carbon exchange. *Plant, Cell & Environment* **27**, 1239–1256. doi:10.1111/j.1365-3040.2004.01231.x</jrn>

<jrn>Schansker G, Tórh SZ, Holzwarth AR, Garab G (2014) Chlorophyll *a* fluorescence: beyond the limits of the Q_A model. *Photosynthesis Research* **120**, 43–58. doi:10.1007/s11120-013-9806-5</jrn>

<jrn>Schreiber U, Schliwa U, Bilger W (1986) Continuous recording of photochemical and non-photochemical chlorophyll fluorescence quenching with a new type of modulation fluorometer. *Photosynthesis Research* **10**, 51–62. doi:10.1007/BF00024185</jrn>

<jrn>Schreiber U, Klughammer C, Kolbowski J (2012) Assessment of wavelength-dependent parameters of photosynthetic electron transport with a new type of multi-color PAM chlorophyll fluorometer. *Photosynthesis Research* **113**, 127–144. doi:10.1007/s11120-012-9758-1</jrn>

<jrn>Smith WK, Berry ZC (2013) Sunflecks? *Tree Physiology* **32**, 1062–1065.</jrn>

<jrn>Stirbet A, Govindjee (2012) Chlorophyll *a* fluorescence induction: a personal perspective of the thermal phase, the J–I–P rise. *Photosynthesis Research* **113**, 15–61. doi:10.1007/s11120-012-9754-5</jrn>

<jrn>Strasser RJ, Srivastava A, Govindjee (1995) Polyphasic chlorophyll *a* fluorescence transient in plants and cyanobacteria. *Photochemistry and Photobiology* **61**, 32–42. doi:10.1111/j.1751-1097.1995.tb09240.x</jrn>

<jrn>Strasser RJ, Tsimilli-Michael M, Qiang S, Goltsev V (2010) Simultaneous *in vivo* recording of prompt and delayed fluorescence and 820 nm reflection changes during drying and after rehydration of the resurrection plant *Haberlea rhodopensis*. *Biochimica et Biophysica Acta* **1797**, 1313–1326. doi:10.1016/j.bbabio.2010.03.008</jrn>

<jrn>Suggett DJ, Oxborough K, Baker NR, MacIntyre HL, Kanna TM, Geider RJ (2003) Fast repetition rate and pulse amplitude modulation chlorophyll *a* fluorescence measurements for assessment of photosynthetic electron transport in marine phytoplankton. *European Journal of Phycology* **38**, 371–384. doi:10.1080/0967026031000161265 5</jrn>

<jrn>Suggett DJ, MacIntyre HL, Kana TM, Geider RJ (2009) Comparing electron transport with gas exchange: parameterising exchange rates between alternative photosynthetic currencies for eukaryotic phytoplankton. *Aquatic Microbial Ecology* **56**, 147–162. doi:10.3354/ame01303</jrn>

<jrn>Suorsa M, Järvi S, Grieco M, Nurmi M, Pietrzykowska M, Rantala M, Kangasjärvi S, Paakkarinen V, Tikkanen M, Jansson S, Aro E-M (2012) PROTON GRADIENT REGULATION5 is essential for proper acclimation of *Arabidopsis* photosystem I to naturally and artificially fluctuating light conditions. *The Plant Cell* **24**, 2934–2948. doi:10.1105/tpc.112.097162</jrn>

Publisher: CSIRO; Journal: FP:Functional Plant Biology
Article Type: research-article; Volume: ; Issue: ; Article ID: FP17024
DOI: 10.1071/FP17024; TOC Head:

<jrn>Terao T, Katoh S (1996) Antenna sizes of photosystem I and photosystem II in chlorophyll *b*-deficient mutants of rice. Evidence for an antenna function of photosystem II centers that are inactive in electron transport. *Plant & Cell Physiology* **37**, 307–312. doi:10.1093/oxfordjournals.pcp.a028947</jrn>

<jrn>Terashima I, Inoue I (1984) Comparative photosynthetic properties of palisade tissue chloroplasts and spongy tissue chloroplasts of *Camellia japonica* L.: ffunctional adjustment of the photosynthetic apparatus to light environment within a leaf. *Plant & Cell Physiology* **25**, 555–563.</jrn>

<jrn>Tikkanen M, Pippo M, Suorsa M, Sirpiö S, Mulo P, Vainonen J, Vener AV, Allahverdiyeva Y, Aro E-M (2006) State transitions revisited: a buffering system for dynamic low light acclimation of *Arabidopsis*. *Plant Molecular Biology* **62**, 779. doi:10.1007/s11103-006-9044-8</jrn>

<jrn>Vredenberg W (2015) A simple routine for quantitative analysis of light and dark kinetics of photochemical and non-photochemical quenching of chlorophyll fluorescence in intact leaves. *Photosynthesis Research* **124**, 87–106. doi:10.1007/s11120-015-0097-x</jrn>

<jrn>Walker DA (1981) Secondary fluorescence kinetics of spinach leaves in relation to the onset of photosynthetic carbon assimilation. *Planta* **153**, 273–278. doi:10.1007/BF00383899</jrn>

<edb>Walker DA, Sivak MN, Cerovic ZG (1984) The relationships between photosynthetic carbon metabolism and chlorophyll *a* fluorescence. In 'Advances in photosynthesis research Vol. III'. (Eds C Sybesma, M Nijhoff) pp. 645–648. (Dr W Junk Publishers: The Hague)</edb>

<jrn>Ware MA, Belgio E, Ruban AV (2015) Photoprotective capacity of non-photochemical quenching in plants acclimated to different light intensities. *Photosynthesis Research* **126**, 261–274. doi:10.1007/s11120-015-0102-4</jrn>

<jrn>Watling JR, Robinson SA, Woodrow IE, Osmond CB (1997) Responses of rainforest understorey plants to excess light during sunflecks. *Australian Journal of Plant Physiology* **24**, 17–23. doi:10.1071/PP96074</jrn>

<jrn>Wyber RA, Malenovsky Z, Ashcroft MB, Osmond B, Robinson SA (2017) Do daily and seasonal trends in leaf solar induced fluorescence reflect changes in photosynthesis, growth or light exposure? *Remote Sensing*, in press.</jrn>

Fig. 1. The prototype LIFT/FRR instrument operated with the Q_A flash to achieve near full reduction of Q_A for non-intrusive, continuous monitoring of chlorophyll fluorescence parameters (including F_o, F_mQ_A, $\phi_{PSII}Q_A$ and σ_{PSII}) Data are from single flashes applied at ~60 cm to dark adapted spinach leaves grown in full sunlight.

Fig. 2. The prototype LIFT/FRR operated with the 'double flash' protocol in which the Q_A flash is followed by a longer PQ flash to obtain spot measurements for internal calibration of Q_A flash data against values for F_oPQ, F_mPQ and $\phi_{PSII}PQ$ attained with fully reduced PQ pool during the prolonged transient. Measurements with the PQ flash are highly correlated 1 : 1 with values from PAM (see later Fig. 5*c*). Data are from single flashes applied at ~60 cm to dark adapted spinach leaves grown in full sunlight.

Fig. 3. The O-J-I-P phases of a chlorophyll a fluorescence induction transient from attached, dark adapted leaves of spinach plants. Fluorescence yields at O and J are proportional to F_oQ_A and F_mQ_A, from the Q_A flash in Fig. 1*a*, *b*. Fluorescence yields at O and P are proportional to F_oPQ and F_mPQ estimated from the PQ flash

Publisher: CSIRO; Journal: FP:Functional Plant Biology
Article Type: research-article; Volume: ; Issue: ; Article ID: FP17024
DOI: 10.1071/FP17024; TOC Head:

in Fig. 2 *a, b*. Data from the same dark adapted, sun grown spinach leaves used in Figs 1 and 2; means ± s.e. (n = 6).

Fig. 4. Continuous monitoring of a brief (~1 s) strong, PAM-analogous WL pulse in the dark with the Q_A flash (Fig. 1). Measured values of (*a*) F_oQ_A, F_mQ_A and (*b*) $\phi_{PSII}Q_A$ from FRR fit to each Q_A flash were used to estimate photosynthetic parameters (*c–e*) from the FRR model. Individual Q_A flash profiles for colour coded data points before, during and after the WL pulse are shown as a function of time during the SQ_A phase (linear time scale) and RQ_A phase (log10 time scale) (*f–h*). These colour-coded profiles illustrate abolition of variable fluorescence during the pulse (red trace) due to complete reduction of both Q_A and PQ pools, followed by the complexity in the RQ_A phase that underlies FRR model fit to reveal the ~ 25 s kinetic for recovery of all photosynthetic parameters to pre-flash conditions.

Fig. 5. Relationships between (*a*) LIFT/FRR-based $\phi'_{PSII}PQ$ and $\phi'_{PSII}Q_A$, (*b*) between PAM-based $\phi'_{PSII}PAM$ and LIFT/FRR based $\phi'_{PSII}Q_A$, and (*c*) between LIFT/FRR based $\phi'_{PSII}PQ$ and PAM-based $\phi'_{PSII}PAM$ measured on adjacent areas of uniformly illuminated leaves during light response curves. Data in (c), with 1:1 relationship and high R^2 indicate functional equivalence of LIFT and PAM techniques performed under conditions of full reduction of PQ pool. Applying the regression equation between $\phi'_{PSII}PQ$ and $\phi'_{PSII}Q_A$ in (*a*) to calculate electron transport rates based on photosynthetic efficiency under conditions of reduced PQ pool gives Q_A flash-based estimates of electron transport rates that are virtually identical to those based on PAM measurements (*d*).

Fig. 6. Combination of Q_A flashes for continuous minimally-intrusive monitoring of fluorescence with near fully reduced Q_A and interspersed PQ flashes to obtain maximum fluorescence yield (with fully reduced PQ pool) as reference for PAM-equivalent estimates of ETR and NPQ. Screen captures from spinach leaves (*a*) showing the slowing of F_mPQ relaxation (and other parameters) on transition from room light (~7 µmol photons m^{-2} s^{-1} fluorescent room light with ~2 µmol photons m^{-2} s^{-1} nFR) to darkness due to over-reduction of the PQ pool in the PQ flash; (*b*) continuous monitoring with the combined protocol is essentially non-intrusive in the dark, and (*c*), capturing the transient in fluorescence parameters during stepwise increases in PFD in a light response curve with spinach leaves.

Fig. 7. PAM-equivalent assays NPQ in (*a*) shade leaves of avocado using spot measurements from the LIFT/FRR 'double flash' (Fig. 2*a*) and saturating pulse of PAM at 60 s intervals during photosynthetic induction (from dark to 100 µmol photons m^{-2} s^{-1}, then returned to dark) and (*b*) correlations between continuously monitored F'_mQ_A (fully reduced Q_A) and LIFT spot measurements of both F'_mPQ (in avocado) and F'_mWL (in *Arabidopsis*) measured with fully reduced PQ. (*c*) Correlations between NPQ measured by LIFT referenced to F'_mWL and NPQ measured by PAM in *Arabidopsis* parent *pgr5 bkg* and NPQ impaired *pgr5* mutant during induction in 1000 µmol photons m^{-2} s^{-1} WL and (*d*) expansion of the first 150 s of NPQ induction comparing 5–6 s time resolution of Q_A flash-based measurements in *pgr5 bkg*, and 2–3 s time resolution in *pgr5*, with PAM data (saturating pulses every 30 s; PAM data mean ± s.e., n = 3).

Fig. 8. Comparisons of the relative impact of LIFT and PAM assay systems on chlorophyll fluorescence yield and photochemical efficiency of PSII. The same leaves of shade grown spinach were continuously monitored by the Q_A flash of LIFT for F_o and F_mQ_A (*a*, *c*) and $\phi_{PSII}Q_A$ (*b*, *d*), and with repeated spot measurements using

Publisher: CSIRO; Journal: FP:Functional Plant Biology
Article Type: research-article; Volume: ; Issue: ; Article ID: FP17024
DOI: 10.1071/FP17024; TOC Head:

the saturating pulse of PAM to measure F_o, F_mPAM and $\phi_{PSII}PAM$ using normal settings (*a*, *b*), or minimal settings (*c*, *d*). Abbreviations: MI, measuring beam intensity; SI, saturating pulse intensity settings for PAM.

Fig. 9. Continuous monitoring of photosynthesis with the Q_A flash, during a sun fleck on a young fully expanded avocado leaf in the shade canopy of a mature tree. Photosynthetic parameters estimated from chlorophyll fluorescence yields averaged from four Q_A flashes and fitted with the FRR model at 5–6 s intervals are shown with three periods of interest (i–iii) identified for discussion. Measured incident PFD and ETR calculated from PFD and measured ϕ'_{PSII} are shown in (*a*); measured F'_mQ_A and $F'Q_A$ in (*b*) and measured ϕ'_{PSII} and NPQ calculated from F'_mQ_A and the regression equation in Fig. 5*b* are shown in (*c*). Measured half times for ETR from $Q_A \rightarrow$ PQ and PQ $\rightarrow$ PSI, and relative oxidation state of the PQ pool estimated from the FRR model are shown in (*d*) and values of σ'_{PSII}, a'_{PSII} and E_k estimated from the FRR model are shown in (*e*). Illustrative examples of individual Q_A flash chlorophyll fluorescence at colour-coded data points in (*b*) are shown in (*f–h*) along with corresponding values of $\phi_{PSII}Q_A$. Note that the SQ_A phase is presented on a linear time base, whereas the RQ_A phase is on a log time base.

Table 1. Nomenclature for differentiation of three classes of chlorophyll fluorescence parameters obtained from LIFT/FRRF from those obtained from the saturating pulse of PAM

Parameter	Definition	Summary of LIFT fluorescence parameters
Q_A flash	LIFT excitation protocol designed to reduce Q_A and to observe the kinetics of electron transport from Q_A to PQ pool and from PQ pool to PSI	SQ_A saturating sequence of 180 flashlets at 50% duty cycle (average excitation power ~6300 μmol photons m^{-2} s^{-1}; 1 μs pulses of 470 nm light applied at 2 μs intervals) followed by RQ_A relaxation sequence of 90 flashlets at exponentially-increasing time intervals
PQ flash	LIFT excitation protocol designed to fully reduce PQ pool, but programmed to fire at predetermined intervals during continual Q_A flash operation.	SPQ saturating sequence of up to 6000 flashlets at 20 μs intervals, followed by relaxation phase (RPQ) of 90 flashlets. Functionally analogous to the saturating pulse of PAM
'Double flash'	LIFT Q_A flash as above followed by a PQ flash as above	Used to 'internally calibrate' Q_A flash parameters against PAM-analogous PQ flash
Ft	Fluorescence transient observed in response to any of the above LIFT/FRRF flash protocols	Fluorescence signal digitised at 10^7 samples s^{-1}, integrated over the length of each flashlet
F_oQ_A	Intrinsic *continuously monitored* fluorescence with fully oxidised Q_A in the dark	FRR fit to Q_A Ft to pre-flash conditions in the dark
F_mQ_A	Maximum *continuously monitored* fluorescence under ambient levels of Q_A and PQ pool reduction	FRR fit to Q_A Ft under ambient levels of Q_A and PQ pool reduction in the dark
F_vQ_A	Variable fluorescence *continuously monitored* in the dark (proportional to reducible Q_A)	$= F_mQ_A - F_oQ_A$
$F'Q_A$	As F_oQ_A but in actinic light	As above but in actinic light
F'_mQ_A	As F_mQ_A but in actinic light	As above but in actinic light
F'_vQ_A	As F_vQ_A but in actinic light	$= F'_mQ_A - F'Q_A$
F_oPQ	*Spot measurement* of intrinsic fluorescence with fully reduced PQ pool in the dark	FRR fit of PQ Ft to pre-flash conditions in the dark (c.f. F_oPAM)
F_mPQ	*Spot measurement* of maximum fluorescence with fully reduced PQ in the dark	FRR fit of PQ Ft with full reduction of PQ pool (c.f. F_mPAM)
F_vPQ	*Spot measurement* of variable fluorescence with fully reduced PQ in the dark	$= F_mPQ - F_oPQ$ (c.f. F_vPAM)
$F'PQ$	As F_oPQ but in actinic light	As above but in actinic light (c.f. $F'PAM$)
F'_mPQ	As F_mPQ but in actinic light	As above but in (c.f. F'_m PAM))
F'_vPQ	As F_vPQ but in actinic light	$= F'_mPQ - F'PQ$ (c.f. F'_vPAM)
F_mWL	*Spot measurement* of maximum fluorescence with fully reduced PQ in the dark	FRR fit to Q_A Ft with fully reduced PQ pool in a strong WL pulse in the dark (c.f. F_mPAM)

Publisher: CSIRO; Journal: FP:Functional Plant Biology
Article Type: research-article; Volume: ; Issue: ; Article ID: FP17024
DOI: 10.1071/FP17024; TOC Head:

F_vWL	*Spot measurement* of variable fluorescence with fully reduced PQ in the dark	= $F_mWL - F_oQ_A$ (c.f. F_vPAM)
F'_mWL	As F_mWL but in actinic light	As above but in actinic light (c.f. F'_mPAM)
F'_vWL	As F_vWL but in actinic light	= $F'_mWL - F'_oQ_A$ (c.f. F'_vPAM)
F_oPAM	Intrinsic fluorescence signal from PAM in the dark	(c.f. F_oPQ)
F_mPAM	Maximum fluorescence from PAM in the dark in a saturating WL pulse to fully reduced PQ	(c.f. F_mWL or F_mPQ)
F_vPAM	Variable fluorescence in the dark from PAM	(c.f. F_vWL or F_vPQ)
F'_oPAM	As F_oPAM but in actinic light	(c.f. F'_oPQ)
F'_mPAM	As F_mPAM but in actinic light	(c.f. F'_mWL or F_mPQ)
F'_vPAM	As F_vPAM but in actinic light	(c.f. F'_vWL or F_vPQ)
$\phi_{PSII}Q_A$	Maximum photochemical efficiency of open PSII centres *continuously monitored* in the dark with ambient levels of Q_A reduction	= $(F_mQ_A - F_oQ_A)/F_mQ_A$
$\phi'_{PSII}Q_A$	As above but in actinic light	= $(F'_mQ_A - F'_oQ_A)/F'_mQ_A$
$\phi_{PSII}PQ$	Maximum photochemical efficiency of open PSII centres in the dark from *spot measurements* with the PQ flash	= F_vPQ/F_mPQ (c.f. F_vPAM/F_mPAM)
$\phi'_{PSII}PQ$	As above in actinic light	= F'_vPQ/F'_mPQ (c.f. F'_vPAM/F'_mPAM)
$\phi_{PSII}WL$	Maximum photochemical efficiency of open PSII centres *continuously monitored* in the dark with the Q_A flash	= F_vWL/F_mWL (c.f. F_vPAM/F_mPAM)
$\phi'_{PSII}WL$	As above in actinic light	= F'_vWL/F'_mWL (c.f. F'_vPAM/F'_mPAM)
$\phi_{PSII}PAM$	Maximum photochemical efficiency of open PSII centres in the dark from *spot measurements* in a saturating pulse from PAM	= F_vPAM/F_mPAM (c.f. F_vPQ/F_mPQ)
$\phi'_{PSII}PAM$	As above in actinic light	= F'_vPAM/F'_mPAM (c.f. F_vPQ/F_mPQ)
σ_{PSII}	*Continuously monitored* functional absorption cross-section of PSII in the dark	Numerical fit of FRR model to Ft of Q_A flash
σ'_{PSII}	As above but in actinic light	As above
a_{PSII}	*Continuously monitored* optical absorption cross-section of PSII (antenna size) in the dark	= $\sigma_{PSII}/\phi_{PSII}$
a'_{PSII}	As above but in actinic light	= $\sigma'_{PSII}/\phi_{PSII}$
τ_1	*Continuously monitored* time constant of electron transport from Q_A to PQ pool	Numerical fit of Q_A flash Ft to FRR model, roughly corresponding to first phase of RQ_A fluorescence relaxation kinetics
τ_2	*Continuously monitored* time constant of electron transport from PQ pool to PSI	Numerical fit of Q_A flash Ft to FRR model, roughly corresponding to second phase of RQ_A fluorescence relaxation kinetics
E_k	*Continuously monitored* half saturation PFD for ETR	FRR model simulation of instantaneous light response curve

Table 2. Relative impact of LIFT/FRR and PAM assays on the photochemical efficiency of PSII in a shade grown avocado leaf measured in the dark before and after a light response curve (mean ± s.e.; *n* = 6)

Maximum photochemical efficiencies of PSII	Before light response curve	After light response curve	% Decline
$\phi_{PSII}Q_A$ (LIFT Q_A flash)	0.694 ± 0.005	0.683 ± 0.003	1.6
$\phi_{PSII}PQ$ (LIFT PQ flash)	0.802 ± 0.002	0.778 ± 0.002	2.9
$\phi_{PSII}PAM$ (PAM saturating pulse)	0.763 ± 0.002	0.654 ± 0.006	14.3

Publisher: CSIRO; Journal: FP:Functional Plant Biology
Article Type: research-article; Volume: ; Issue: ; Article ID: FP17024
DOI: 10.1071/FP17024; TOC Head:

Table 3. LIFT/FRR measurements of the functional absorption cross-section of PSII (σ_{PSII}) and estimates of relative antenna size in wild-type and antenna mutants of *Arabidopsis* and barley (mean ± s.e.)

Values for mutants as a percent of wild types are bracketed (in italics); footnotes refer to *in vitro* literature estimates

Species, genotype and growth irradiance (μmol m^{-2} s^{-1})	σ_{PSII}	$a_{PSII} = \sigma_{PSII}/\phi_{PSII}$
Arabidopsis Col (~120)	333 ± 9 (*n* = 6)	396 ± 11 (*n* = 6)
Arabidopsis asLhcb2–12 (~120)	256 ± 6 (*n* = 8) (*77*%)	299 ± 7 (*n* = 8) (*76*%)[A, B]
Arabidopsis Col (~60)	469 ± 44 (*n* = 7)	548 ± 51 (*n* = 7)
Arabidopsis ch1–3 Lhcb5 (~60)	107 ± 11 (*n* = 4) (*23*%)	125 ± 13 (*n* = 4) (*23*%)[C]
Barley wild type (ANU) (~1000)	335 ± 20 (*n* = 5)	408 ± 26 (*n* = 5)
Barley *chlorina-f2* (ANU) (~1000)	117 ± 7 (*n* = 7) (*35*%)	152 ± 9 (*n* = 7) (*37*%) [D]
Barley wild type (Fz-J) (60–400)	191 ± 9 (*n* = 8)	256 ± 13 (*n* = 8)
Barley *chlorina-f2* (Fz-J) (60–400)	77 ± 5 (*n* = 8) (*40*%)	114 ± 7 (*n* = 8) (*45*%)[D]

[A] ~75% (Andersson *et al*. 2003); [B] 60% (Belgio *et al*. 2014); [C] ~35% (Kim *et al*. 2009); [D] ~20% (Cleland and Melis 1987; Harrison *et al*. 1993).

Table 4. LIFT/FRR measurements of the functional absorption cross-section of PSII (σ_{PSII}) and optical absorption cross-section (a_{PSII}) in *Arabidopsis* grown at low PFD transferred to sun, and spinach grown in the sun, then transferred to low PFD (mean ± s.e.)

Change in values as a percent are bracketed (in italics)

Genotype, growth conditions and PFD	σ_{PSII} ($Å^2$/PSII centre)	a_{PSII} (= $\sigma_{PSII}/\phi_{PSII}$) ($Å^2$/PSII centre)
Arabidopsis Col growth chamber(~80–120 μmol m^{-2} s^{-1})	368 ± 6 (*n* = 7)	584 ± 29
Arabidopsis Col growth chamber then 10 days sun (~400–1200 μmol photons m^{-2} s^{-1})	288 ± 12 (*n* = 4) (*78*%)	443 ± 10 (*76*%)
Spinach greenhouse sun(~400–1200 μmol photons m^{-2} s^{-1})	339 ± 9 (*n* = 6)	490 ± 13
Spinach greenhouse sun then dim room light for 2 days (~5 μmol photons m^{-2} s^{-1})	381 ± 8 (*n* = 6) (*112*%)	556 ± 12 (*135*%)

Table 5. Decline in functional (σ_{PSII}) and optical (a_{PSII}) absorption cross-sections of PSII in *Arabidopsis* genotypes with increase in PFD during growth

Genotype	Growth PFD (μmol photons m^{-2} s^{-1})			
	60–80	120	60–80	120
	σ_{PSII} ($Å^2$/PSII centre)		a_{PSII} ($Å^2$/PSII centre)	
Wild type *Col* (*n* = 6)	492 ± 29	365 ± 8	593 ± 35	439 ± 13
npq4 (*n* = 5)	461 ± 6	352 ± 16	555 ± 8	424 ± 19
asLhcb2–12 (*n* = 4)	443 ± 13	282 ± 13	533 ± 19	340 ± 17
stn7 (*n* = 4)	556 ± 29	375 ± 6	670 ± 36	464 ± 8
stn7/8 (*n* = 4)	594 ± 35	364 ± 8	715 ± 42	439 ± 10

Table 1: Nomenclature for differentiation of three classes of chlorophyll fluorescence parameters obtained from LIFT/FRRF from those obtained from the saturating pulse of PAM

Parameter	Definition	Summary of LIFT fluorescence parameters
Q_A flash	LIFT excitation protocol designed to reduce Q_A and to observe the kinetics of electron transport from Q_A to PQ pool and from PQ pool to PSI	SQ_A saturating sequence of 180 flashlets at 50% duty cycle (average excitation power ~ 6,300 μmol photons m^{-2} s^{-1}; 1 μs pulses of 470 nm light applied at 2 μs intervals) followed by RQ_A relaxation sequence of 90 flashlets at exponentially-increasing time intervals
PQ flash	LIFT excitation protocol designed to fully reduce PQ pool, but programmed to fire at predetermined intervals during continual Q_A flash operation.	SPQ saturating sequence of up to 6,000 flashlets at 20 μs intervals, followed by relaxation phase (RPQ) of 90 flashlets. Functionally analogous to the saturating pulse of PAM
"double flash"	LIFT Q_A flash as above followed by a PQ flash as above	Used to "internally calibrate" Q_A flash parameters against PAM-analogous PQ flash
Ft	Fluorescence transient observed in response to any of the above LIFT/FRRF flash protocols	Fluorescence signal digitized at 10^7 samples s^{-1}, integrated over the length of each flashlet.
F_oQ_A	Intrinsic *continuously monitored* fluorescence signal with fully oxidized Q_A in the dark	FRR fit to Q_A Ft to pre-flash conditions in the dark
F_mQ_A	Maximum *continuously monitored* fluorescence signal under ambient levels of Q_A and PQ pool reduction.	FRR fit to Q_A Ft under ambient levels of Q_A and PQ pool reduction in the dark
F_vQ_A	Variable fluorescence *continuously monitored* in the dark (proportional to reducible Q_A)	$= F_mQ_A - F_oQ_A$
$F'Q_A$	Intrinsic *continuously monitored* fluorescence signal in actinic light	FRR fit to Q_A Ft to pre-flash conditions in actinic light
F'_mQ_A	Maximum *continuously monitored* fluorescence signal under ambient conditions of Q_A and PQ pool reduction in actinic light	FRR fit to Q_A Ft under ambient conditions of Q_A and PQ pool reduction in actinic light)
F'_vQ_A	Variable fluorescence *continuously monitored* in actinic light (proportional to reducible Q_A)	$= F'_mQ_A - F'Q_A$
F_mWL	*Spot measurement* of maximum fluorescence with fully reduced PQ in the dark	FRR fit to Q_A Ft with fully reduced PQ pool in a strong WL pulse in the dark (c.f., F_mPAM)
F_vWL	*Spot measurement* of variable fluorescence with fully reduced PQ in the dark	$= F_mWL - F_oQ_A$ (c.f., F_vPAM)
F'_mWL	*Spot measurement* of maximum fluorescence with fully reduced PQ in actinic light	FRR fit to Q_A Ft with fully reduced o PQ pool in a strong WL pulse in actinic light (c.f., F'_mPAM)
F'_vWL	*Spot measurement* of variable fluorescence with fully reduced PQ in actinic light	$= F'_mWL - F'_oQ_A$ (c.f., F'_vPAM)
$F_o\,PAM$	Intrinsic fluorescence signal from PAM in the dark	(c.f., F_oPQ)
$F_m\,PAM$	Maximum fluorescence in the dark from PAM in a saturating WL pulse to fully reduced PQ	(c.f., F_mWL or F_mPQ)
$F_v\,PAM$	Variable fluorescence in the dark from PAM	(c.f., F_vWL or F_vPQ)
$F'\,PAM$	Intrinsic fluorescence signal from PAM in actinic light	(c.f., $F'PQ$)
$F'_m\,PAM$	Maximum fluorescence from PAM with fully reduced PQ pool in actinic light	(c.f., F'_mWL or F_mPQ)
$F'_v\,PAM$	Variable fluorescence from PAM in actinic light	(c.f., F'_vWL or F_vPQ)
F_oPQ	*Spot measurement* of intrinsic fluorescence with fully reduced PQ pool in the dark	FRR fit of PQ Ft to pre-flash conditions in the dark (c.f., $F_o\,PAM$)
F_mPQ	*Spot measurement* of maximum fluorescence with fully reduced PQ in the dark	FRR fit of PQ Ft with full reduction of PQ pool (c.f., $F_m\,PAM$)
F_vPQ	*Spot measurement* of variable fluorescence with fully reduced PQ in the dark	$= F_mPQ - F_oPQ$ (c.f., $F_v\,PAM$)

$F'PQ$ F'_mPQ F'_vPQ	*Spot measurement* of intrinsic fluorescence with fully reduced PQ pool in actinic light *Spot measurement* of maximum fluorescence with fully reduced PQ in actinic light *Spot measurement* of variable fluorescence with fully reduced PQ in actinic light	FRR fit to PQ Ft to pre-flash conditions in actinic light (c.f., $F'PAM$) FRR fit to PQ Ft with full reduction of PQ pool (c.f., F'_mPAM)) $= F'_mPQ - F'PQ$ (c.f., F'_vPAM)
$\phi_{PSII}Q_A$	Maximum photochemical efficiency of open PSII centres *continuously monitored* in the dark with ambient levels of Q_A reduction	$= (F_mQ_A - F_oQ_A) / F_mQ_A$
$\phi'_{PSII}Q_A$	As above but in actinic light	$= (F'_mQ_A - F'Q_A) / F'_mQ_A$
$\phi_{PSII}WL$	Maximum photochemical efficiency of open PSII centres *continuously monitored* in the dark with the Q_A flash	$= F_vWL / F_mWL$ (c.f., F_vPAM / F_mPAM)
$\phi'_{PSII}WL$	As above in actinic light	$= F'_vWL / F'_mWL$ (c.f., F'_vPAM / F'_mPAM)
$\phi_{PSII}PAM$	Maximum photochemical efficiency of open PSII centres in the dark from *spot measurements* in a saturating pulse from PAM	$= F_vPAM / F_mPAM$ (c.f., F_vPQ / F_mPQ)
$\phi'_{PSII}PAM$	As above in actinic light	$= F'_vPAM / F'_mPAM$ (c.f., F_vPQ / F_mPQ)
$\phi_{PSII}PQ$	Maximum photochemical efficiency of open PSII centres in the dark from *spot measurements* with the PQ flash	$= F_vPQ / F_mPQ$ (c.f., F_vPAM / F_mPAM)
$\phi'_{PSII}PQ$,	As above in actinic light	$= F'_vPQ / F'_mPQ$ (c.f., F'_vPAM / F'_mPAM)
σ_{PSII}	*Continuously monitored* functional absorption cross section of PSII in the dark	Numerical fit of FRR model to Ft of Q_A flash
σ'_{PSII}	As above but in actinic light	As above
a_{PSII}	*Continuously monitored* optical absorption cross section of PSII (antenna size) in the dark	$= \sigma_{PSII} / \phi_{PSII}$
a'_{PSII}	As above but in actinic light	$= \sigma'_{PSII} / \phi_{PSII}$
τ_1	*Continuously monitored* time constant of electron transport from Q_A to PQ pool	Numerical fit of Q_A flash Ft to FRR model, roughly corresponding to first phase of RQ_A fluorescence relaxation kinetics
τ_2	*Continuously monitored* time constant of electron transport from PQ pool to PSI	Numerical fit of Q_A flash Ft to FRR model, roughly corresponding to second phase of RQ_A fluorescence relaxation kinetics
E_k	*Continuously monitored* half saturation PFD for ETR	FRR model simulation of instantaneous light response curve

Table 2: Relative impact of LIFT/FRR and PAM assays on the photochemical efficiency of PSII in a shade grown avocado leaf measured in the dark before and after a light response curve with sequential exposures of three to six min. in WL at 37, 53, 71, 131, 266, 526, and 60 μmol photons (n = 6 measurements by each assay)

Maximum photochemical efficiencies of PSII	Before light response curve	After light response curve	% decline
$\phi_{PSII}Q_A$ (LIFT Q_A flash)	0.694 ± 0.005	0.683 ± 0.003	1.6
$\phi_{PSII}PQ$ (LIFT PQ flash)	0.802 ± 0.002	0.778 ± 0.002	2.9
$\phi_{PSII}PAM$ (PAM saturating pulse)	0.763 ± 0.002	0.654 ± 0.006	14.3

Table 3: LIFT/FRR measurements of the functional absorption cross section of PSII (σ_{PSII}) and estimates of relative antenna size in wild type and antenna mutants of arabidopsis and barley. Optical absorption cross section (a_{PSII}; antenna size) is estimated using $\phi_{PSII}WL$ data at ANU (fully reduced PQ) and $\phi_{PSII}Q_A$ (fully reduced Q_A) data at Fz-J. Values for mutants as a percent of wild types are shown in italics; superscripted numbers refer to in vitro literature estimates cited in the footnote (mean ± SE).

Species, genotype and growth irradiance (µmol m^{-2} s^{-1})	σ_{PSII}	$a_{PSII} = \sigma_{PSII}/\phi_{PSII}$
Arabidopsis *Col* (~120)	333 ± 9 (n = 6)	396 ± 11 (n = 6)
Arabidopsis *asLhcb2-12* (~120)	256 ± 6 (n = 8) ***77%***	299 ± 7 (n = 8) ***76 %*** [(1)(2)]
Arabidopsis *Col* (~ 60)	469 ± 44 (n = 7)	548 ± 51 (n = 7)
Arabidopsis *ch1-3lhcb5* (~ 60)	107 ± 11 (n = 4) ***23 %***	125 ± 13 (n = 4) ***23 %*** [(3)]
Barley wild type (ANU) (~1000)	335 ± 20 (n = 5)	408 ± 26 (n = 5)
Barley *chlorina-f2* (ANU) (~1000)	117 ± 7 (n = 7) ***35%***	152 ± 9 (n = 7) ***37 %*** [(4)]
Barley wild type (Fz-J) (60 - 400)	191 ± 9 (n = 8)	256 ± 13 (n = 8)
Barley *chlorina-f2* (Fz-J) (60 - 400)	77 ± 5 (n = 8) ***40%***	114 ± 7 (n = 8) ***45 %*** [(4)]

[(1)] ~75% (Andersson *et al.* 2003); [(2)] 60% (Belgio *et al.* 2014); [(3)] ~35% (Kim *et al.* (2008); [(4)] ~20% (Cleland and Melis 1987; Harrison *et al.* 1993)

Table 4: LIFT/FRR measurements of the functional absorption cross section of PSII (σ_{PSII}) and optical absorption cross section (a_{PSII}) in arabidopsis grown at low PFD transferred to sun, and spinach grown in the sun, then transferred to low PFD (mean ± SE). Change in values as a percent are shown in italics.

Genotype, growth conditions and PFD	σ_{PSII}	a_{PSII} (= σ_{PSII} / ϕ_{PSII})
	(Å^2 / PSII center)	
Arabidopsis *Col* growth chamber (~80-120 µmol m^{-2} s^{-1})	368 ± 6 (n = 7)	584 ± 29
" " then 10 d sun (~400-1200 µmol photons m^{-2} s^{-1})	288 ± 12 (n = 4) ***78%***	443 ± 10 ***76%***
Spinach greenhouse sun (~400-1200 µmol photons m^{-2} s^{-1})	339 ± 9 (n = 6)	490 ± 13
" then dim room light (2 d) (~5 µmol photons m^{-2} s^{-1})	381 ± 8 (n = 6) ***112%***	556 ± 12 ***135%***

Table 5: Decline in functional (σ_{PSII}) and optical (a_{PSII}) absorption cross sections of PSII in arabidopsis genotypes with increase in PFD during growth.

Genotype	Growth PFD (µmol photons m^{-2} s^{-1})			
	60-80	120	60-80	120
	σ_{PSII} ($Å^2$/PSII center)		a_{PSII} ($Å^2$/PSII center)	
Wild type *Col* (n=6)	492 ± 29	365 ± 8	593 ± 35	439 ± 13
npq4 (n=5)	461 ± 6	352 ± 16	555 ± 8	424 ± 19
asLhcb2-12 (n=4)	443 ±13	282 ± 13	533 ± 19	340 ± 17
stn7 (n=4)	556 ± 29	375 ± 6	670 ± 36	464 ± 8
stn7/8 (n=4)	594 ± 35	364 ± 8	715 ± 42	439 ± 10

Figure 1: The prototype LIFT/FRR instrument operated with the Q_A flash to achieve near full reduction of Q_A for non-intrusive, continuous monitoring of chlorophyll fluorescence parameters (including F_o, F_mQ_A, $\phi_{PSII}Q_A$ and σ_{PSII}) Data are from single flashes applied at ~60 cm to dark adapted spinach leaves grown in full sunlight.

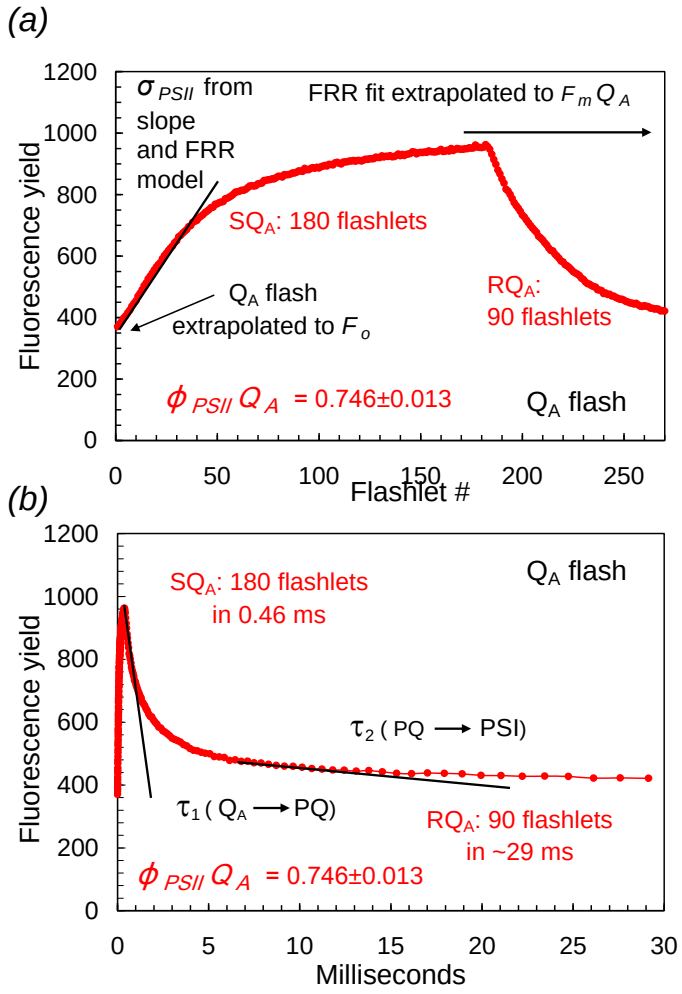

Figure 2: The prototype LIFT/FRR operated with the "double flash" protocol in which the Q_A flash is followed by a longer PQ flash to obtain spot measurements for internal calibration of Q_A flash data against values for F_oPQ, F_mPQ and $\phi_{PSII}PQ$ attained with fully reduced PQ pool during the prolonged transient. Measurements with the PQ flash are highly correlated 1:1 with values from PAM (Fig. 3*c*). Data are from single flashes applied at ~60 cm to dark adapted spinach leaves grown in full sunlight.

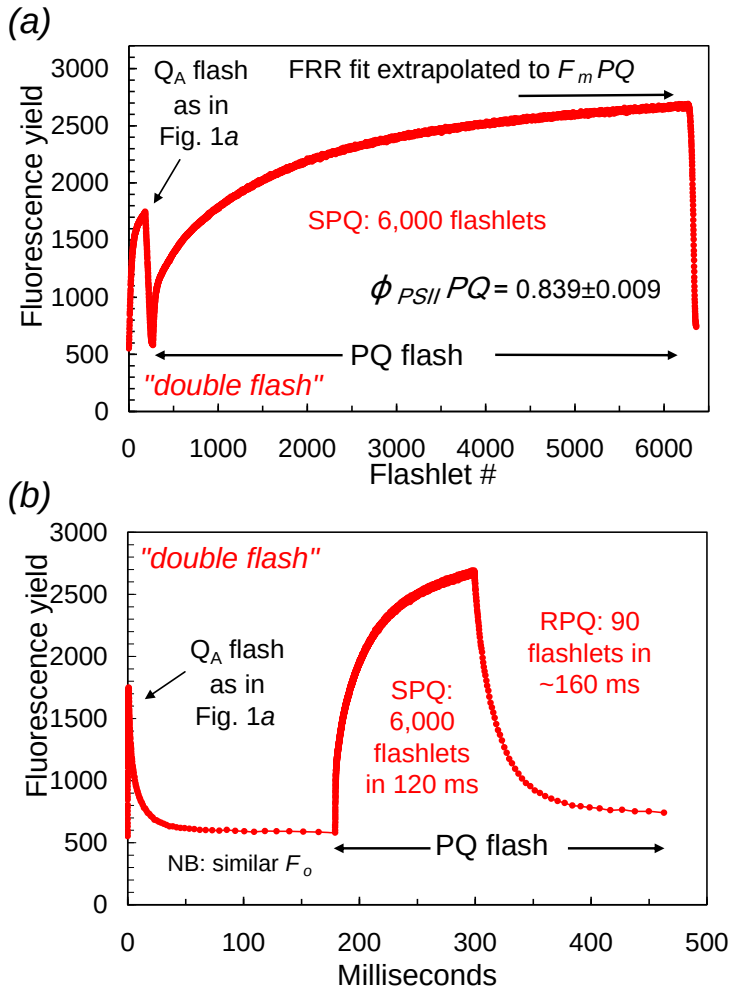

Figure 3: The O-J-I-P phases of a chlorophyll *a* fluorescence induction transient from attached, dark adapted leaves of spinach plants. Fluorescence yields at O and J are proportional to F_oQ_A and F_mQ_A, from the Q_A flash in Figs. 1*a*, *b*. Fluorescence yields at O and P are proportional to F_oPQ and F_mPQ estimated from the PQ flash in Figs. *4a*, *b*. Data from the same dark adapted, sun grown spinach leaves used in Figs. 1 and 3; means ± SE (n = 6).

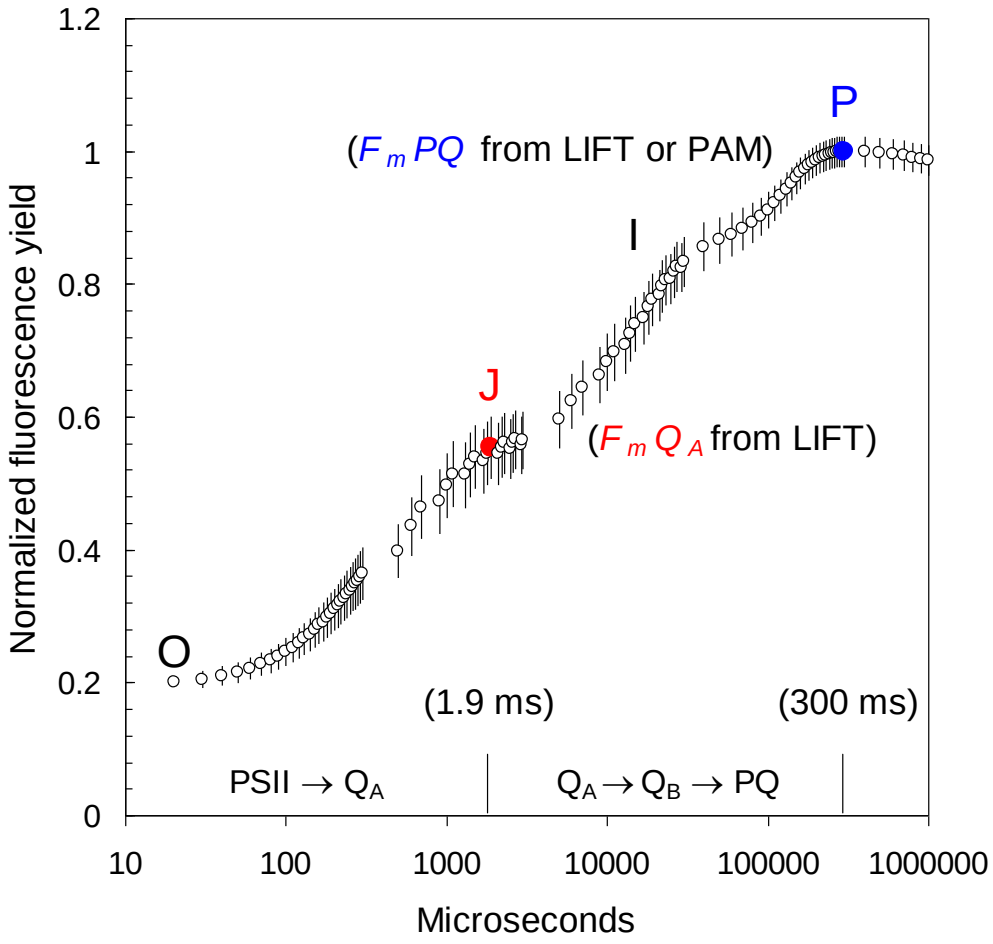

Figure 4: Continuous monitoring of a brief (~1 s) strong, PAM-analogous WL pulse in the dark with the Q_A flash (Fig. 1). Measured values of (***a***) F_oQ_A, F_mQ_A and (***b***) $\phi_{PSII}Q_A$ from FRR fit to each Q_A flash were used to estimate photosynthetic parameters (***c***)-(***e***) from the FRR model. Individual Q_A flash profiles for colour coded data points before, during and after the WL pulse are shown as a function of time during the SQ_A phase (linear time scale) and RQ_A phase (log_{10} time scale) (***f-h***). These colour-coded profiles illustrate abolition of variable fluorescence during the pulse (red trace) due to complete reduction of both Q_A and PQ pools, followed by the complexity in the RQ_A phase that underlies FRR model fit to reveal the ~ 25 s kinetic for recovery of all photosynthetic parameters to pre-flash conditions.

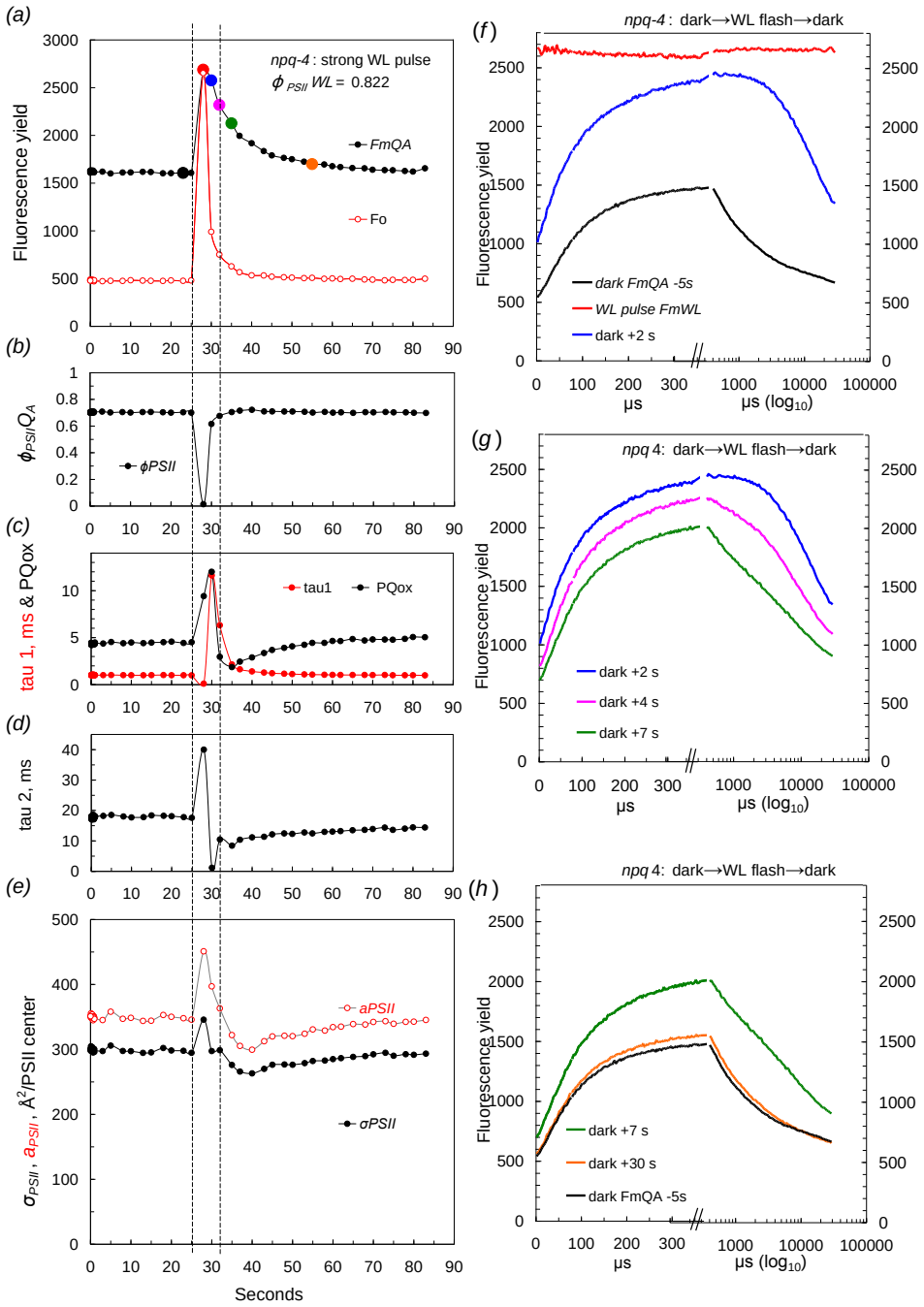

Figure 5: Relationships between (*a*) LIFT/ FRR-based $\phi'_{PSII}PQ$ and $\phi'_{PSII}Q_A$, (*b*) between PAM-based $\phi'_{PSII}PAM$ and LIFT/FRR based $\phi'_{PSII}Q_A$, and (*c*) between LIFT/FRR based $\phi'_{PSII}PQ$ and PAM-based $\phi'_{PSII}PAM$ measured on adjacent areas of uniformly illuminated leaves during light response curves. Data in (*c*), with 1:1 relationship and high R^2 indicate functional equivalence of LIFT and PAM techniques performed under conditions of full reduction of PQ pool. Applying the regression equation between $\phi'_{PSII}PQ$ and $\phi'_{PSII}Q_A$ in (*a*) to calculate electron transport rates based on photosynthetic efficiency under conditions of reduced PQ pool gives Q_A flash-based estimates of electron transport rates that are virtually identical to those based on PAM measurements (*d*).

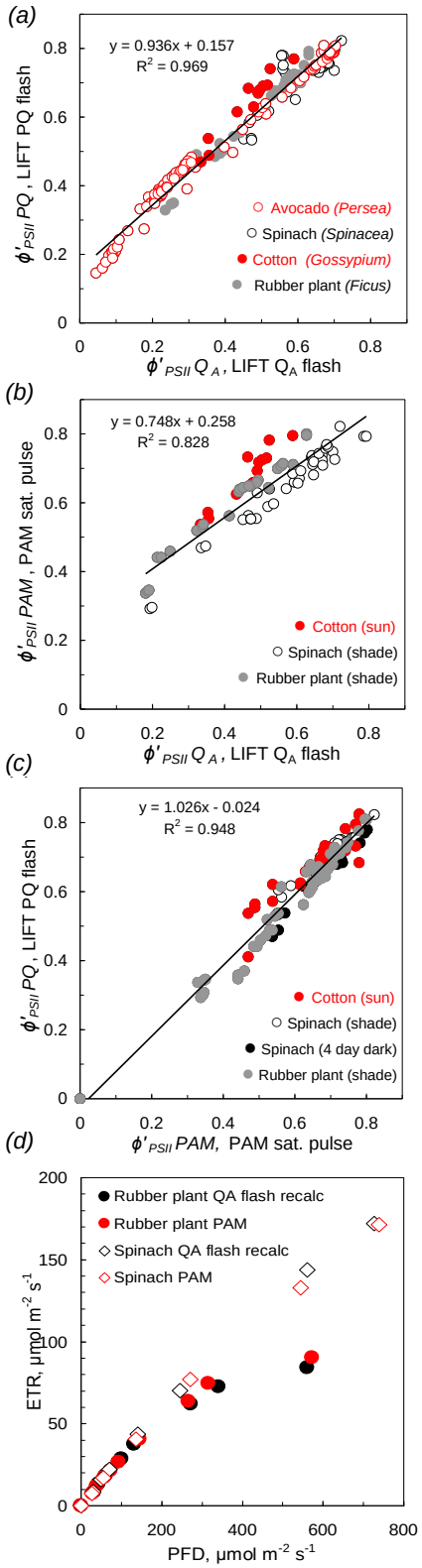

Figure 6: Combination of Q_A flashes for continuous minimally-intrusive monitoring of fluorescence with near fully reduced Q_A and interspersed PQ flashes to obtain maximum fluorescence yield (with fully reduced PQ pool) as reference for PAM-equivalent estimates of ETR and NPQ. Screen captures from spinach leaves (*a*) showing the slowing of F_mPQ relaxation (and other parameters) on transition from room light (~7 µmol photons m^{-2} s^{-1} fluorescent room light with ~2 µmol photons m^{-2} s^{-1} nFR) to darkness due to over-reduction of the PQ pool in the PQ flash; (*b*) continuous monitoring with the combined protocol is essentially non-intrusive in the dark, and (*c*), capturing the transient in fluorescence parameters during stepwise increases in PFD in a light response curve with spinach leaves.

(*a*)

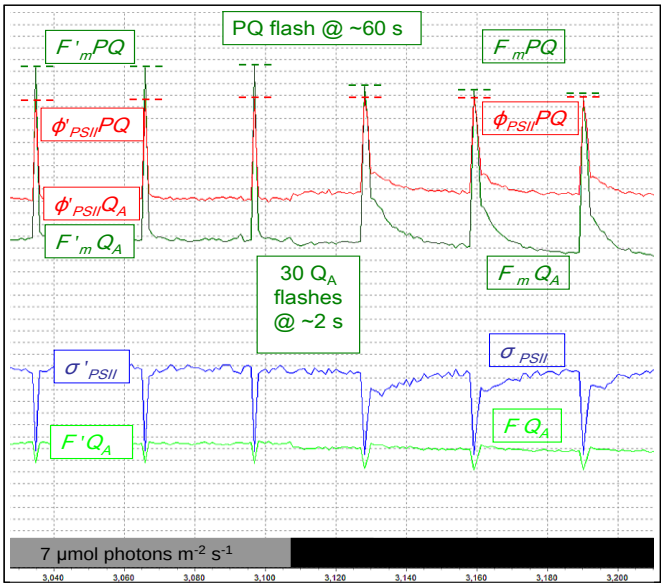

(*b*)

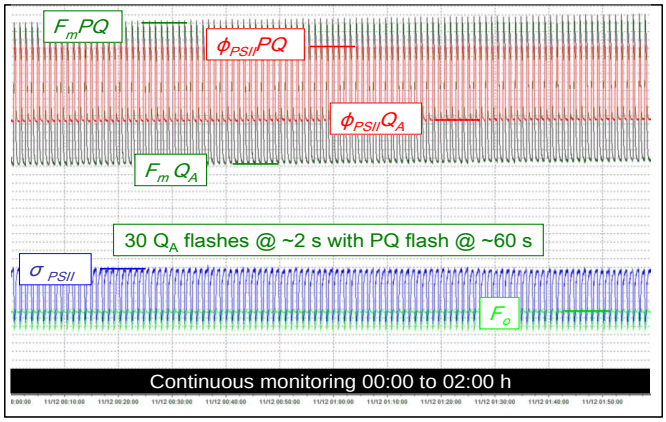

(*c*)

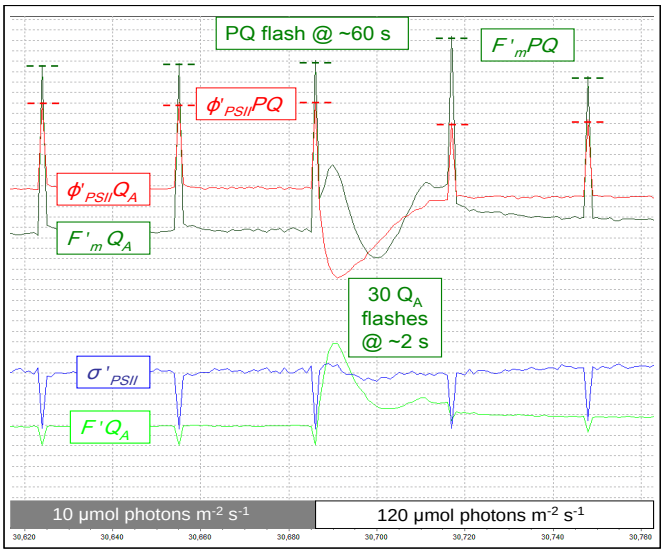

Figure 7: PAM-equivalent assays NPQ in (***a***) shade leaves of avocado using *spot measurements* from the LIFT/FRR "double flash" (Fig. 4*a*) and saturating pulse of PAM at 60 s intervals during photosynthetic induction (from dark to 100 µmol photons m^{-2} s^{-1}, then returned to dark) and (***b***) correlations between continuously monitored F'_mQ_A (fully reduced Q_A) and LIFT *spot measurements* of both F'_mPQ (in avocado) and F'_mWL (in *Arabidopis*) measured with fully reduced PQ. (***c***) Correlations between NPQ measured by LIFT referenced to F'_mWL and NPQ measured by PAM in arabidopsis parent *pgr5 bkg* and NPQ impaired *pgr5* mutant during induction in 1,000 µmol photons m^{-2} s^{-1} WL and (***d***) expansion of the first 150 s of NPQ induction comparing 5-6 s time resolution of Q_A flash-based measurements in *pgr5 bkg*, and 2-3 s time resolution in *pgr5*, with PAM data (saturating pulses every 30 s; PAM data mean ± SE; n = 3).

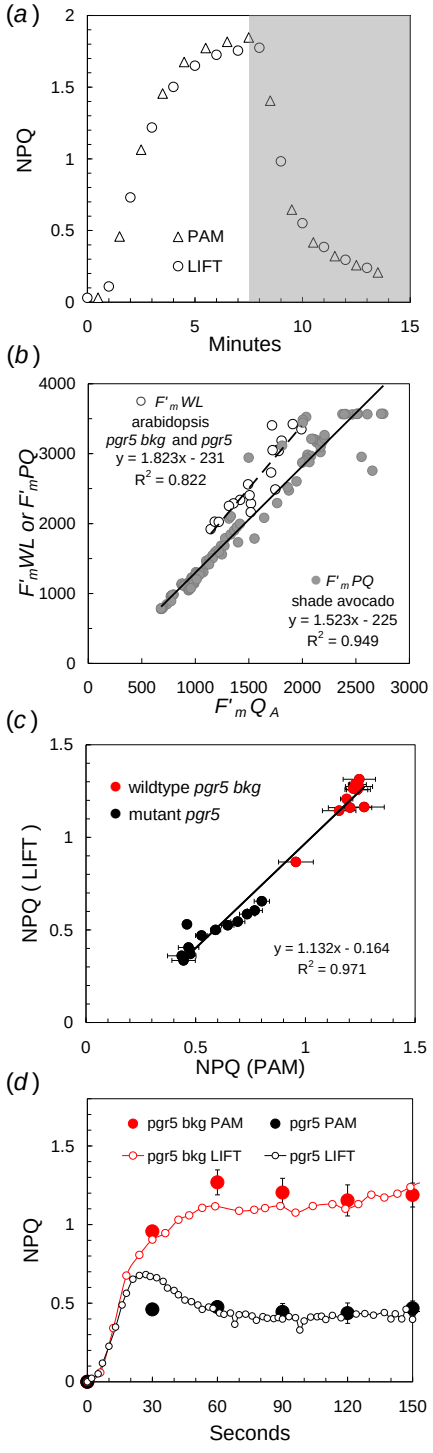

Figure 8: Comparisons of the relative impact of LIFT and PAM assay systems on chlorophyll fluorescence yield and photochemical efficiency of PSII. The same leaves of shade grown spinach were continuously monitored by the Q_A flash of LIFT for F_o and F_mQ_A (***a, c***) and ϕ_{PSII} Q_A (***b, d***), and with repeated spot measurements using the saturating pulse of PAM to measure F_o, F_mPAM and $\phi_{PSII}PAM$ using normal settings (***a, b***), or minimal settings (***c, d***). (MI = measuring beam intensity; SI = saturating pulse intensity settings for PAM).

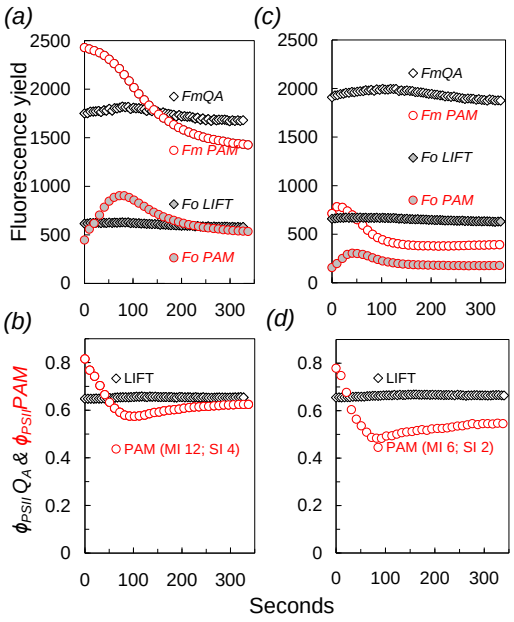

Figure 9: Continuous monitoring of photosynthesis with the Q_A flash, during a sun fleck on a young fully expanded avocado leaf in the shade canopy of a mature tree. Photosynthetic parameters estimated from chlorophyll fluorescence yields averaged from four Q_A flashes and fitted with the FRR model at 5-6 s intervals are shown with three periods of interest (i-iii) identified for discussion. Measured incident PFD and ETR calculated from PFD and measured ϕ'_{PSII} are shown in (*a*); measured F'_mQ_A and $F'Q_A$ in (*b*) and measured ϕ'_{PSII} and NPQ calculated from F'_mQ_A and the regression equation in Fig. 5*b* are shown in (*c*). Measured half times for ETR from $Q_A \rightarrow$ PQ and PQ $\rightarrow$ PSI, and relative oxidation state of the PQ pool estimated from the FRR model are shown in (*d*) and values of σ'_{PSII}, a'_{PSII} and E_k estimated from the FRR model are shown in (*e*). Illustrative examples of individual Q_A flash chlorophyll fluorescence at colour-coded data points in (*b*) are shown in (*f-h*) along with corresponding values of $\phi_{PSII}Q_A$. Note that the SQ_A phase is presented on a linear time base, whereas the RQ_A phase is on a log time base.